

# The Origin of Planetary Ring Systems

S. CHARNOZ, R. M. CANUP, A. CRIDA, AND L. DONES

## 18.1 Introduction

The origin of planetary rings is one of the least understood processes related to planet formation and evolution. Whereas rings seem ubiquitous around giant planets, their great diversity of mass, structure and composition is a challenge for any formation scenario. Satellite destruction by cometary impacts and meteoroid bombardment seem to be key processes leading to the very low-mass rings of Uranus, Neptune and Jupiter. By contrast, moon destruction is unlikely to produce Saturn’s much more massive rings recently, so they still represent a strong challenge for astronomers.

Recent advances in our understanding of ring and satellite formation and destruction suggest that these processes are closely interconnected, so that rings and satellites may be two aspects of the same geological system. Indeed, rings may not be only beautiful planetary ornaments, but, possibly, an essential step in the process of satellite formation, at least for the small and mid-sized moons. These recent advances have taken advantage of the many tantalizing results from the Cassini mission, as well as advances in numerical simulation techniques. However, no single theory seems able to explain the origin of the different planetary rings known in our Solar System, and it now seems evident that rings may result from a variety of processes like giant collisions, tidal stripping of comets or satellites, as well as planet formation itself. Understanding rings appears to be an important step toward understanding the origin and evolution of planetary environments.

Most work on the origin of rings has been devoted to Saturn, and somewhat less to the rings of Jupiter, Uranus and Neptune. So our chapter will be mainly focused on the case of Saturn. However, processes that are common to all rings or particular to those of Saturn will be clearly delineated. In order to build any theory of ring formation it is important to specify physical processes that affect the long-term evolution of rings, as well as to describe the different observations that any ring formation model should explain. This is the topic of section 18.2. In section 18.3, we focus our attention on Saturn’s rings and their main properties, and then discuss the pros and cons of a series of ring formation

models. We also discuss the link between rings and satellites. In section 18.4, we extend the discussion to the other giant planets (Jupiter, Uranus, and Neptune). Section 18.5 is devoted to new types of rings –the recent discovery of rings orbiting small outer Solar System bodies (Centaur), and the possible rings around extrasolar planets (“exo-rings”). In section 18.6, we conclude and try to identify critical observations and theoretical advances needed to better understand the origin of rings and their significance in the global evolution of planets.

## 18.2 Ring Processes

### 18.2.1 Basics of Ring Dynamics

Rings, as we know them in our Solar System, are disks of solid particles, in contrast to protoplanetary disks, which have a gaseous component. With the exception of tenuous “dust” rings, which can extend far from their planets, planetary rings occur within  $\approx 2.5$  planetary radii, a location prone to intense tidal forces. In dense rings, particles have nearly-keplerian orbits<sup>1</sup>, and they cross the midplane of the rings twice per orbit, with a vertical component of the velocity equal to the orbital velocity times the sine of their inclination angle. The link between the thickness  $H$  of a ring and the relative velocity of particles  $\sigma_v$  is therefore  $\sigma_v = H\Omega$ , where  $\Omega$  is the keplerian angular velocity. By analogy between the agitation of the particles and that of the molecules of a gas, one refers to a dynamically *cold* system when  $\sigma_v$  is small compared to the orbital velocity  $V_{\text{orb}}$ , and to a dynamically *hot* system otherwise. With  $V_{\text{orb}} = r\Omega$  (where  $r$  is the distance to the center of the planet), the ratio  $\sigma_v/V_{\text{orb}} = H/r \equiv h$  is the aspect ratio.

Unlike in a gas, collisions in a debris disk dissipate energy. Hence, if collisions are frequent (as is the case in Saturn’s rings, but not in debris disks around stars), the relative velocity drops quickly, and the ring becomes thin and dynamically *cold*. The aspect ratio  $h$  of Saturn’s rings is about  $10^{-7}$ ,

<sup>1</sup> Because a planet’s rotation makes it somewhat nonspherical, the potential felt by a ring particle is not exactly that of a point mass at the center of the planet. The fractional difference  $f$  from a keplerian potential is of order  $J_2(R/r)^2$ , where the zonal harmonic coefficient  $J_2$  is in the range 0.004–0.016 for the four giant planets,  $R$  is the equatorial radius of the planet, and  $r$  is the distance of the ring from the center of the planet. Thus  $f = \mathcal{O}(10^{-3} - 10^{-2})$  for planetary rings.

—  
This chapter is from the book Planetary Rings Systems, edited by Matthew S. Tiscareno and Carl D. Murray. This version is free to view and download for personal use only. Not for redistribution, re-sale or use in derivative works. ©Cambridge University Press, [www.cambridge.org/9781107113824](http://www.cambridge.org/9781107113824).

making this system the thinnest natural structure known and the best example of a dynamically cold disk. The local physical thickness  $H$  of Saturn’s main rings is generally about 10 m (Zebker and Tyler, 1984; Colwell et al., 2009), comparable to the physical size of the largest ring particles themselves (Ferrari and Reffet, 2013). This means that Saturn’s rings are probably as cold as possible, *i.e.*, they have reached their minimum state of internal energy. This is analogous to a thermodynamically evolved system that has evolved over many cooling timescales.

In a dynamically hot system, the relative velocities are much larger than the escape velocity from the surface of an object in the system. Hence, gravitational focusing has little effect, collisions do not permit accretion, and self-gravity has a negligible effect. By contrast, in a dynamically cold system, particles significantly deflect each other’s trajectories, allowing for more collisions, potentially allowing accretion. To quantify the effects of self-gravity in a near-keplerian disk, the  $Q$  parameter is used (Toomre, 1964):

$$Q = \frac{\Omega \sigma_r}{3.36 G \Sigma}, \quad (18.1)$$

where  $\sigma_r$  is the particles’ radial velocity dispersion,  $G$  is the gravitational constant, and  $\Sigma$  is the surface density of solids.  $Q$  is the ratio of dispersive forces to gravitational forces. For  $Q > 2$ , self-gravity can be neglected. When  $Q < 2$ , spiral density wakes can appear, and when  $Q < 1$ , the system is gravitationally unstable and clumping is expected.

However, even in a gravitationally unstable system, there can be forces that oppose clumping of solid particles – tides from the central body. Tidal forces are a differential effect of gravitation that tend to stretch any object in the gravitational field of another one, along the axis between the two centers of mass<sup>2</sup>. If tides are very strong (because the object exerting them is very massive, or the distance to this object is very small), they affect the shape of the object being perturbed. Tides can even be as strong as the gravity at the surface of an object. In the absence of internal strength, the object is destroyed. Roche (1849) studied the deformation of a liquid blob in orbit around a planet, and found that there is no equilibrium solution (*i.e.*, the liquid blob is dispersed), if it is closer to the center of the central planet than

$$r_R = 2.45 R_p (\rho_p / \rho_l)^{1/3}, \quad (18.2)$$

where  $R_p$  is the radius of the planet,  $\rho_p$  is its density, and  $\rho_l$  is the density of the liquid. This limit is called the Roche radius. One can compute it in various ways (considering the separation of two spheres, for instance, or the loss of a test particle from the surface of a rigid object), but this only changes the leading numerical coefficient from  $\simeq 1.5$  to  $\simeq 2.5$  (Weidenschilling et al., 1984). The notion of the Roche limit is robust, whereas its precise location may depend on the physical process to consider (accretion, destruction, splitting, etc.), as well as on the material density of the ring particles. As the ratio of the densities only enters Eq. (18.2) as the one-third power, the Roche radius is roughly 2.5 plan-

<sup>2</sup> For example, it is well known that the Earth’s oceans are elongated along an axis pointing (roughly) toward the Moon due to our satellite’s gravity.

etary radii if the ring material’s density is comparable to the planet’s density.

Taking the density of porous ice for the material constituting the rings ( $\approx 800 \text{ kg/m}^3$ ), one finds that the Roche limit around Saturn is at  $r_R \approx 140,000 \text{ km}$ , near the clumpy F ring. Hence, Saturn’s rings, dominated by water ice, can never aggregate and form a single moon: they are inside their Roche radius. Such a Roche-interior disk is very interesting because self-gravity can be the dominant process, but yet the ring structure persists and no permanent accretion is possible.

### 18.2.2 Spreading of Rings

Whenever two particles in a ring interact, the total angular momentum is conserved. If the interaction changes their velocity vector, they may exchange angular momentum. As inner particles have a larger velocity than the outer ones, interactions generally result in a transfer of angular momentum from the inner to the outer ones. This is similar to a sheared viscous fluid: friction between faster and slower rings tends to slow the former down, and accelerate the latter. Even if rings are not fluid, and do not have a viscosity in the strict meaning of this word, the angular momentum exchanges, being proportional to the shear, can be modeled by a viscosity effect. In keplerian dynamics, the viscous torque exerted by the region inside a circle of radius  $r_0$  on the outside is given by (see e.g. Pringle, 1981):

$$\Gamma_\nu = 3\pi \Sigma \nu r_0^2 \Omega_0, \quad (18.3)$$

where  $\nu$  is the kinematic viscosity, and  $\Omega_0$  is the orbital frequency at  $r_0$ .

Angular momentum conservation and mass conservation combined yield the variations of the surface density  $\Sigma$  (see, e.g., Salmon et al., 2010; Pringle, 1981):

$$\frac{\partial \Sigma}{\partial t} = \frac{3}{r} \frac{\partial}{\partial r} \left[ \sqrt{r} \frac{\partial (\nu \Sigma \sqrt{r})}{\partial r} \right] \quad (18.4)$$

Using a constant, uniform viscosity  $\nu$ , Lynden-Bell and Pringle (1974) derived the equations for the evolution of an initially infinitesimally narrow gaseous disk. However, the equation driving any astrophysical disk controlled by viscosity and gravity is formally the same, so it is also used in the context of planetary ring evolution. As the innermost regions orbit faster, they transfer angular momentum to the outer ones, which increases the orbital radius of the outer material, and decreases that of the inner material. The ring spreads, while angular momentum flows outwards. The frontier separating inward accretion and outward spreading moves outwards with time. The theoretical final state is that of lowest energy: all the mass has fallen to the center, while all the angular momentum is carried by an infinitesimally small particle at infinity.

In Roche-interior rings, the interaction between particles cannot be modeled by a constant, uniform viscosity. Ring particles exchange angular momentum when they collide, but also due to their gravitational interaction during close encounters. The larger the surface density of the rings (*i.e.*, the smaller the Toomre parameter  $Q$ ), the stronger these

exchanges can be. Daisaka et al. (2001) provide a complete description of this phenomenon and a complex prescription for the viscosity  $\nu$ , which depends on  $Q$  and  $\Sigma$ .

According to Daisaka et al. (2001), in the gravity-dominated regime (massive rings), the viscosity  $\nu$  of the rings is proportional to their mass squared. The characteristic time for viscous spreading of a ring of radius  $r_R$  is  $t_\nu = r_R^2/\nu \approx \frac{1}{30}\mu^{-2}T_R$ , where  $\mu = M_{\text{rings}}/M_p$  (where  $M_{\text{rings}} \approx \pi\Sigma r_R^2$  is the mass of the rings and  $M_p$  is the mass of the planet), and  $T_R$  is the orbital period at  $r_R$ . As  $d\mu/dt = -\mu/t_\nu$ , one finds  $d\mu/d\bar{t} = -30\mu^3$ , with  $\bar{t} = t/T_R$ . The solution of this differential equation is (Crida and Charnoz, 2014):

$$\mu(t) = \frac{1}{\sqrt{60\bar{t} + \mu_0^{-2}}}. \quad (18.5)$$

Clearly, memory of the initial ring mass through  $\mu_0$  is erased once  $\bar{t} \gg 1/60\mu_0^2$ , and in the long term,  $\mu(t) \approx (60\bar{t})^{-1/2}$ , independent of  $\mu_0$ . Around Saturn, with  $t = 4.5$  billion years, this gives  $\mu = 8 \times 10^{-8}$ . Note that this is a slowly varying function, so the result varies by only a factor of 2 from 3.5 billion years ago to the present. This is illustrated by 1D numerical simulations of the evolution of the rings (Eq. (18.4)) performed by Salmon et al. (2010) who have studied the global, long-term evolution of rings and of their density profile using the prescription of Daisaka et al. (2001) for the viscosity (figure 18.2). Figure 18.1 illustrates the erasure of the initial conditions mentioned in the previous calculation: whatever the initial mass, the final state has a mass of few  $\times 10^{22}$  g after 4 Gyr.

Today, estimates of the ring mass based on surface densities derived from density waves (mostly in the A ring) give a mass of  $\simeq 4 \times 10^{22}$  g, corresponding to  $\mu = 7 \times 10^{-8}$ . The agreement between the model of ring spreading and the measured mass suggests that Saturn’s rings could be primordial, and that their present mass may not be the result of their formation process, but rather of their evolution during Solar System history. In particular, it means that Saturn’s rings could have been much more massive in the past, by almost arbitrary amounts, and that the initial mass of Saturn’s rings has a lower limit but not an upper limit. Alternatively one could argue that Saturn’s rings are much younger than the Solar System, and that the observed coincidence between the mass of today’s rings and the asymptotic mass of a self-gravitating disk is just a matter of luck. Future measurements of the rings’ current mass, expected during the final orbits of Cassini, as well as analysis of the current flux of meteoroid bombardment by the Cosmic Dust Analyzer team, may provide important constraints relevant to these issues. Nonetheless, the viscous calculations above allow for the possibility of an almost arbitrarily large initial ring mass, and thus open new doors for explaining their formation, as we will see in section 18.3.3.7.

Variable viscosity also helps to maintain sharp ring structures. The decrease of  $\nu$  when  $\Sigma$  drops makes the ring have sharp edges, which move slower than in the case of a uniform viscosity. The densest regions spread faster, but the spreading slows down dramatically as soon as the self-gravity ef-

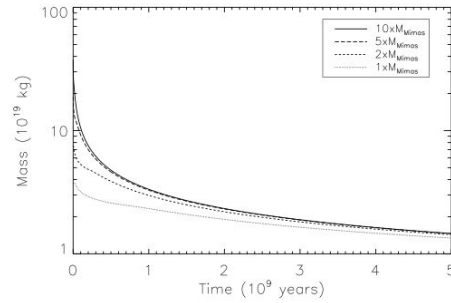


**Figure 18.1** Mass of Saturn’s rings as a function of time, starting with different initial values of the rings’ mass. The material flows either into Saturn’s atmosphere or leaves the Roche limit. Whatever the initial mass, the final mass is always nearly the same, after 2 Gyr of evolution. The mass is controlled by the value of  $Q \simeq 2$  everywhere. This calculation includes the ring mass lost to the satellite system. Adapted from Salmon et al. (2010).

fects, responsible for angular momentum transfer, decrease. In fact, in the simulations of Salmon et al. (2010), the surface density profile of the rings converges naturally to a profile which makes  $Q = 2$  everywhere (where  $Q$  is defined by Eq. (18.1)). This occurs because in the Daisaka et al. (2001) prescription, the gravitational component of viscosity is switched off where  $Q > 2$ , causing a drop in  $\nu$  which almost freezes the rings’ profile. This behavior is typical of self-gravitating disks where there is a feedback mechanism between self-gravity and heating: if  $Q < 2$  then the disk heats up because of the appearance of shock waves and spiral arms, thus increasing  $Q$ . Conversely when  $Q > 2$  internal dissipation (here in collisions) helps the disk to cool down and thus  $Q$  decreases. The existence of an asymptotic state for Saturn’s rings by maintaining  $Q \simeq 2$  everywhere is not limited to planetary rings, but seems to be a general property of self-gravitating disks, and is also expected for circumstellar disks (see, e.g., Rice and Armitage, 2009).

Such a profile is in qualitative agreement with the observed one, and Saturn’s rings are indeed marginally gravitationally unstable. The “peak” seen in figure 18.3 at  $5 \times 10^9$  yr could be associated with the B ring (whereas its surface density is still a matter of debate), and the long tail may be associated with the A ring. Interestingly, this study suggests that there is at most a factor 2 to 3 difference between the surface densities of the two rings.

Of course, the detailed structure of Saturn’s rings is not explained by this simple viscous model. In particular, it does not explain the existence of the C ring, the origin of the Cassini Division, and numerous small-scale structures in the rings such as plateaus and ramps. Other processes clearly sculpt the rings, including bombardment and ballistic transport (see Chapter 9), as well as ring-satellite interactions.

### 18.2.3 Perturbation by Satellites

Exchange of angular momentum via gravity are not limited to particle – particle interactions. Satellites orbiting beyond the rings have a gravitational influence on the particles, de-

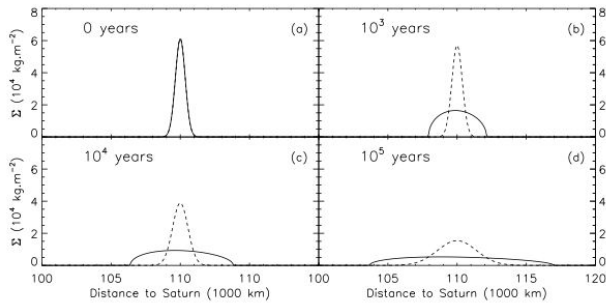


**Figure 18.2** Ring surface density at different evolution times for variable (solid line) and constant (dashed line) viscosities. (a) Initial profile. (b) At 1000 years of evolution. (c) At  $10^4$  years of evolution. (d) At  $10^5$  years of evolution. The disk with variable viscosity spreads faster and does not keep the original shape of the density profile. Adapted from Salmon et al. (2010).

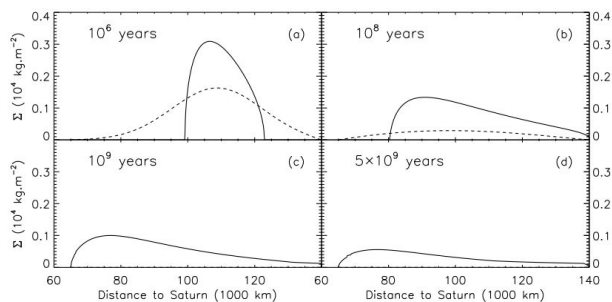


**Figure 18.3** Ring surface density at different evolution times with variable (solid line) and constant (dashed line) viscosities. (a) At 1 Myr of evolution. (b) At 100 Myr of evolution. (c) At 1 Gyr of evolution. (d) At 5 Gyr of evolution. The disk with constant viscosity disperses in 1 Gyr, while the disk with variable viscosity remains massive over 5 Gyr with an inner density peak and lower densities further out. Adapted from Salmon et al. (2010).

flect their trajectories, and on average take angular momentum from them. Computing this deflection and integrating over all the rings, Lin and Papaloizou (1979) found that the total torque felt by a satellite whose mass ratio to the central planet is  $\mu_s$  and orbital radius is  $r$  is given by:

$$\Gamma_L = \frac{8}{27} \mu_s^2 \Sigma r^4 \Omega^2 \Delta^{-3} \quad (18.6)$$

where  $\Delta = (r - r_{\text{rings}})/r$  is the normalized distance between the satellite and the outer edge of the rings, and is assumed to be small (also see Goldreich and Tremaine (1980)). This expression is only valid when the satellite is close to the ring system ( $\Delta \lesssim 0.1$ , see Meyer-Vernet and Sicardy, 1987, their Fig. 8).

This formula is fundamental in ring-satellite interactions. First, satellites close to the rings receive a positive torque, which makes them migrate outwards, at a decreasing speed as  $\Delta$  increases. As this happens, angular momentum is removed from the rings, slowing down their outward spreading. If the viscous torque  $\Gamma_\nu$  (see above) is smaller than this so-called Lindblad torque  $\Gamma_L$ , outward spreading is thwarted and the ring's outer edge can be confined. This is presently

the case around Saturn: e.g., the outer edge of the A ring at 136,700 km is confined by the interaction at a 7:6 resonance with the coorbital moons Janus and Epimetheus, and the outer edge of the B ring is confined by the 2:1 resonance with Mimas. This illustrates that if, in the history of the system, some massive satellites have existed near the rings, they will have perturbed the spreading of the rings and thus their overall evolution.

## 18.2.4 Modified Accretion at the Roche Limit

Because they are dynamically very cold, and their spreading almost stops once  $Q > 2$ , Saturn's rings are maintained in a marginally gravitationally unstable state (e.g., Ward, 1984). As rings spread beyond the Roche radius, they have a natural tendency to clump, and planetary tides become too weak to prevent this natural effect of self-gravity in a dynamically very cold system. It is therefore expected that elongated aggregates of ring particles will form, whose shape is the Roche lobe. The Roche lobe is the region within which the gravitational attraction of a body dominates over the differential attraction of the central planet, and its radial width is given by the Hill radius,  $R_h = a(\mu_s/3)^{1/3}$ , where  $a$  is the distance to the planet. Loosely bound aggregates are therefore very fragile. A high-speed collision can deliver enough energy to unbind the particles, but slow collisions are constructive, and as such a rubble pile can dissipate some impact energy in deformation and compaction. The further they migrate outwards, the larger, the more spherical, and the more resistant to disruption such rubble piles become. Tides can also modify two-body accretion. A particle near the Roche limit nearly fills its Hill sphere, as the definitions of  $R_h$  and  $r_R$  combine into  $R/R_h \approx 0.6(r_R/a)$ , where  $R$  is the particle radius. Two colliding particles must remain inside their mutual Hill sphere in order to remain gravitationally bound to each other. This imposes severe constraints on the geometry of encounters necessary for accretion (and the closer to Saturn, the more severe they are). Canup and Esposito (1995) find that tidally modified accretion between objects differing in size may occur inside the Roche limit, but accretion between equal-sized bodies is prevented. This results in a bimodal size distribution with big bodies remaining on near-circular orbits (but prevented from accreting), co-existing with clouds of tiny particles on more eccentric and inclined orbits. Collisions between big bodies may result in the formation of rings like Saturn's F ring close to the Roche limit, as was shown recently (Hyodo and Ohtsuki, 2015).

## 18.3 Rings of Saturn

### 18.3.1 Surface Density and Mass

The mass of Saturn's rings is a key quantity that constrains models of their origin. We do not yet have a dynamical measurement of the mass of the entire ring system, although the Cassini radio science experiment is expected to determine this quantity during the last year of the mission in

2017. At present, we have measurements of the surface mass density,  $\Sigma$  of the rings at a variety of locations, primarily in the outermost main ring, the A ring, where numerous waves launched by nearby satellites are present. Surface densities in regions where dynamical values are not available are sometimes estimated by assuming that the surface density of the rings is proportional to the optical depth, whose radial profile is measured by occultations across the whole ring system. However, the assumed proportionality requires that the internal density of ring particles and their size-frequency distribution is the same in different regions. As we discuss below, this condition is not always satisfied in the rings (Tiscareno et al., 2013b; Hedman and Nicholson, 2016).

Saturn’s satellites, particularly the “ring moons” Prometheus, Pandora, Janus, Epimetheus, Atlas, Pan and Daphnis as well as the innermost “classical” satellite, Mimas, perturb the rings at locations where a resonance condition is satisfied. In most cases, the perturbations are in the ring plane and cause tightly wound spiral density waves. At a particularly strong resonance, a gap can form. For instance, the Mimas 2:1 Inner Lindblad Resonance (ILR) marks the outer edge of Saturn’s B ring. The rings also harbor a few vertical corrugations known as spiral bending waves, which are excited by moons with (slightly) inclined orbits. As an example, both the Mimas 5:3 density wave and the Mimas 5:3 bending wave are prominent features in the outer A ring. In this part of the A ring, ring particles complete roughly five orbits around Saturn for every three orbits of Mimas. However, the resonance condition also involves the precession rate of the ring particles (positive, i.e., prograde, for apsides and negative, i.e., retrograde, for nodes). Precession splits the resonance, so the 5:3 Inner Vertical Resonance, at which the bending wave is excited, lies some 400 km interior to the 5:3 ILR, at which the density wave is excited.

Density and bending waves can be used to determine the rings’ surface density  $\Sigma$  because their wavelengths are proportional to  $\Sigma$ . As described above, the A ring is the region where the rings’ surface density is best known, as it contains numerous resonances with small moons. From the wave structure the derived surface density is about 40 g/cm<sup>2</sup> (Tiscareno et al., 2007) for the A ring. A recent study (Hedman and Nicholson, 2016) suggests that the B ring’s surface density  $\Sigma$  is between 40 and 140 g/cm<sup>2</sup>. As the optical depth  $\tau$  in much of the B ring is vastly larger than that in the A ring (by roughly a factor of 10, see Colwell et al. (2009)), the inferred surface density of the B ring implies a smaller value of  $\Sigma/\tau$  there. This, in turn, implies that the effective ring particle size is smaller in the B ring, and/or the particles there have smaller internal densities than in the A ring. Hedman and Nicholson (2016) infer that the mass of the B ring is about  $\frac{1}{2}$  to  $\frac{2}{3}$  that of Mimas, and that the total mass of the rings is, at most, comparable to that of Mimas. On the other hand, Larry Esposito (personal communication, 2016) maintains that the five waves studied by Hedman and Nicholson do not sample the B ring adequately, and that the total mass of the ring system might be significantly greater than that of Mimas (Robbins et al., 2010). See Chapter 3 for a discussion on the rings’ opacity and surface density.

### 18.3.2 Composition and Age

Since spacecraft have not directly sampled the particles in Saturn’s main rings, we must use reflection spectra and color to get some indication of their composition. In general, ring particles are similar to the nearby moons, at least on their surfaces. However, some small spectroscopic differences have been identified, and the rings are somewhat redder than the moons (Filacchione et al., 2014). Saturn’s rings are predominantly water ice and therefore bright (Nicholson et al., 2008); by comparison, the macroscopic particles in the jovian, uranian, and neptunian rings are dark (their albedos are small). Color variations across Saturn’s rings may indicate varying composition, possibly due in part to the effects of the interplanetary dust that bombards them and darkens the particles. It is likely that Saturn’s ring particles have rough, irregular surfaces resembling frost more than solid ice. There is good indication that the particles are under-dense (internal densities  $\ll 1$  g/cm<sup>3</sup>, Zhang et al. (2017)), supporting the idea of ring particles as temporary rubble piles. These slowly spinning particles collide gently with collision velocities of just mm/sec. The composition of Saturn’s rings, with more than 90 to 95% water ice, seems to be in strong contrast with some of Saturn’s satellites (Titan, Dione, and Enceladus), which are approximately half-rock, half-ice mixtures, roughly as expected for a solar abundance of solid material. Because bombardment of the rings by silicate-rich micrometeoroids increases their rock content over time, the rings’ current composition implies that they were essentially pure ice when they formed.

Ring-satellite interactions can lead to evolution on timescales much shorter than the age of the Solar System. The expected rate of transfer of angular momentum from the rings to the satellites (section 18.2.3) implies that several of the moons such as Prometheus and Pandora were spawned from the rings  $\ll 100$  Myr ago (Goldreich and Tremaine, 1982; Lissauer et al., 1984; Poulet and Sicardy, 2001; Charnoz et al., 2010). The angular momentum gained by the moons is lost by the rings, and is predicted to cause collapse of the A ring to its inner edge in 100 Myr.

The vast expanse of Saturn’s rings presents an enormous target for impact by interplanetary dust grains. These hypervelocity collisions can erode ring particles and cause loss of ring material to Saturn’s atmosphere (Cook and Franklin, 1970; Morfill et al., 1983; Northrop and Connerney, 1987; Cuzzi and Durisen, 1990). The same impacts can cause the rings’ structure and composition to evolve due to the exchange of ejecta (“ballistic transport”) between different parts of the rings (Ip, 1983, 1984; Lissauer et al., 1984; Durisen, 1984; Durisen et al., 1989, 1992, 1996; Doyle et al., 1989; Cuzzi and Durisen, 1990; Durisen, 1995; Cuzzi and Estrada, 1998; Latter et al., 2014; Estrada et al., 2015) [also see section 17.3.1 in the review by Charnoz et al. (2009b)]. Even in the absence of ballistic transport, accretion of interplanetary dust, which has a low albedo (Ishiguro et al., 2013), should darken the rings (Doyle et al., 1989; Elliott and Esposito, 2011). Unfortunately, the timescales on which these effects operate are uncertain, largely because the rate at which interplanetary projectiles strike the rings (Tis-

careno et al., 2013a) is still uncertain. See Chapter 9 for a discussion of this issue. Recent measurements from the Cassini spacecraft (the Cosmic Dust Analyzer experiment, CDA hereafter) seem to show that meteoritic bombardment could be intense enough so that it may have loaded the rings with several times their own mass over the age of the Solar System (see Chapter 9 for more details). However, the CDA results remain unpublished, and the time variation of the bombardment rate over the lifetime of the rings is unknown. If the CDA results are confirmed and their derived bombardment rates are viewed as typical of past rates, they may imply a ring age much smaller than the age of the Solar System. However, these results are still uncertain.

In principle, limits on the age of Saturn’s rings can be derived from observations of craters on the moons. If young ( $\ll 4$  Gyr) surface ages were derived for the moons, it would hint at young rings as well because of the strong interactions of the rings with the satellites out to Mimas.

The time during which craters have accumulated on a satellite can be calculated if the rate of impact of bodies of different sizes is known, and if the characteristics of the impactors (size, density, velocity, etc.) can be related to the sizes of the observed craters (see section 18.4.2). In recent years, Saturnian satellite ages have been estimated from crater densities by, among others, Zahnle et al. (2003); Kirchoff and Schenk (2009); Dones et al. (2009), and Di Sisto and Zanardi (2016). All of these studies assume that ecliptic comets (also called Centaurs in the region of the giant planets) are the primary impactors. The estimated satellite ages are generally billions of years, with the notable exception of Enceladus’s active south polar region (Porco et al., 2006). At first glance, these “crater ages” argue for old rings. However, the method is not well-calibrated, because we do not have independent knowledge of the size-frequency distribution of the small ecliptic comets ( $\mathcal{O}(0.1\text{--}10$  km diameter)) that are believed to produce most of the craters seen. In fact, on the surface of Rhea and on Dione’s cratered plains, there are more observed craters larger than 6 km than expected in 4.5 Gyr (Di Sisto and Zanardi, 2016); either the assumed population of Centaurs should be revised (perhaps many more Centaurs struck the rings in the early Solar System, see section 18.3.3.3), or another reservoir of impactors is needed.

Ćuk et al. (2016) investigated the dynamical evolution of the mid-sized saturnian moons due to tides. They infer that the moons have migrated little. Tethys and Dione probably did not cross their 3:2 resonance, but the system likely did cross a Dione-Rhea 5:3 resonance and a Tethys-Dione secular resonance. These crossings would have happened recently: within the past 100 Myr for  $Q_p = 1500$  (Lainey et al., 2012, see Eq. (18.8) below). Ćuk et al. (2016) suggested that a previous generation of moons underwent an orbital instability, perhaps due to a solar evection resonance, leading to collisions between them. Today’s moons would have reaccreted from the debris (at locations that allow for the Dione-Rhea 5:3 resonance crossing, but not the Tethys-Dione 3:2), and at least the current rings would presumably be young, although Ćuk et al. (2016) do not address this issue in detail. This model implies that most craters on the

moons were formed by the debris, with impacts taking place at much lower speeds than applies for impacts by comets. While still speculative, this model is interesting because it opens a possibility of forming rings recently, since collisions of icy moons might happen at high enough velocities to be completely destructive (i.e., collision velocities substantially greater than the escape velocities of the colliding bodies, Movshovitz et al. (2016)). However the fate of the debris and whether it could yield the current mid-sized satellites and the rings (and their unique compositions) has not been quantitatively investigated, and would appear dynamically challenging (see section 18.3.3.9 for more details). Further, this model requires a pre-existing system of inner mid-sized satellites, and thus it seems plausible that there could have been a pre-existing ring system as well. Even if a recent large-scale dynamical modification of the inner Saturnian system did occur, the original system mass and compositional trends could possibly reflect a much earlier, perhaps even primordial, epoch of formation. Such issues merit further consideration.

Collisions between similar-sized moons also occur in the Crida and Charnoz (2012) model, which suggests that the regular satellites within Titan’s orbit formed from a series of giant impacts involving roughly equal-sized bodies on nearly-circular orbits. In this scenario, though, the collisions are not destructive but constructive. Still, the debris of these collisions would generate secondary impacts on the target, and possibly on other satellites. Much work remains to be done to determine whether these scenarios can be distinguished from the one discussed above, in which the largest craters are made by comets and planetocentric debris makes only smaller craters (Alvarellos et al., 2005).

### 18.3.3 Models for the Origin of Saturn’s Rings

That debris orbiting interior to the Roche limit at Saturn would remain dispersed in a ring, rather than accumulating into one or more moons, can be understood from the basic principles described above. However, two questions have proved harder to answer: first, what was the source of the material comprising the current main rings at Saturn, and second, why is Saturn’s ring system so much more massive than those of the other gas giants?

During the final stages of Saturn’s formation, the planet was likely surrounded by a circumsaturnian disk containing both gas and solids (rock and ice). Such a disk is a natural birthplace for Titan, as well as some, or maybe all, of the other regular Saturnian satellites out to Iapetus. Initially Saturn would have been much larger than it is at present due to the energy of its accretion (e.g., Pollack et al., 1977). But so long as the planet contracted to within the Roche limit for ice while its disk was still present (which appears plausible, e.g. Pollack et al., 1977; Marley et al., 2007; Fortney et al., 2007), one would expect there to have been an evolving ring of material near the disk’s inner edge.

The lifetime of a ring particle orbiting within a gaseous disk is generally short, because the velocity differential between the pressure-supported gas and the keplerian motion of the particle acts as a drag on the particle’s motion that

causes it to spiral inward and eventually collapse onto the planet. Thus it seems likely that hypothetical primordial ring systems formed within Saturn’s circumplanetary disk were lost. Yet Saturn’s rings must have formed in an environment that allowed them to survive until the current time. The original ring system must have had a mass comparable to or greater than the current ring mass,  $\geq \text{few} \times 10^{22}$  g, and a composition of essentially pure ice, given that the current rings are  $> 90\%$  water ice, despite continuous exposure to external bombardment that over time increases their rock content (e.g., Cuzzi et al., 2010; Cuzzi and Estrada, 1998, also see section 18.3.2). Finally, whatever event(s) produced Saturn’s rings did not produce a comparably large and long-lived ring system around Jupiter, Uranus, or Neptune. It has been proposed (Crida and Charnoz, 2012) that Uranus and Neptune did have early massive ring systems that were somehow lost while Saturn’s massive rings were not, as we describe in section 18.4.2. Simultaneously satisfying this set of constraints for Saturn’s rings is challenging, and a variety of origin models have been proposed. Below we briefly describe these models, focusing in particular on developments occurring since the Charnoz et al. (2009b) review was published.

### 18.3.3.1 Condensation Within a Satellite-Forming Disk

The idea that Saturn’s rings could represent material left over from the protosatellite disk that never coagulated into a satellite, also known as the condensation model, was developed by Pollack (1975) and Pollack et al. (1977) (see Sec. 4.1 in Charnoz et al., 2009b, for additional discussion). In this model, the rings are unaccreted remnants from the same disk of gas and solids that gave rise to the regular satellites. A first challenge is the survival of such a ring against gas drag. For a dense ring, drag by a gas disk can be described as a shear stress on the disk surfaces, resulting in a ring decay timescale (e.g., Goldreich and Ward, 1973; Harris, 1984):

$$\begin{aligned} \tau_{gd} &= 14 Re \left( \frac{\Sigma}{\Sigma_g} \right) \left( \frac{GM_p}{c^3} \right) \\ &\sim 10^2 \text{ yr} \left( \frac{Re}{10^2} \right) \left( \frac{\Sigma/\Sigma_g}{0.03} \right) \left( \frac{200 \text{ K}}{T} \right)^{3/2}, \end{aligned} \quad (18.7)$$

where  $Re$  is the Reynolds number (uncertain, but likely in the range of 50 to 500; e.g., Weidenschilling and Cuzzi, 1993), and  $\Sigma_g$  is the gas surface density,  $c$  is the thermal velocity of the gas molecules, and  $T$  is the gas temperature. For a disk whose gas surface density is substantially higher than its surface density of solids (as would be the case for a solar composition disk), the implied lifetime of a condensed ring is then short compared to the likely lifetime of the gas disk, which could be  $\geq 10^6$  yr.

Low-temperature condensation would generally be expected to produce a rock-ice ring reflecting bulk solar abundances, inconsistent with the essentially pure ice composition needed for consistency with Saturn’s rings. A clever solution to this problem was proposed by Pollack (1976), who argued that as the disk cooled, silicates in the inner

disk would condense before the ices did. If these silicates were lost to gas drag decay, subsequent condensation of ices as the disk cooled further would yield an ice ring. A condensation origin of Saturn’s rings thus requires that (1) ice condensation is delayed until after the earlier-formed rocky ring has been removed, and (2) ice condensation occurred concurrently with the dispersal of the gas disk, so that the resulting ice ring survived. The first is plausible given that timescales in Eqs. (18.7) may be short compared to disk cooling timescales (e.g. Charnoz et al., 2009b). However, (2) appears to require a coincidence.

The condensation model remains an interesting idea, but the lack of a quantitative model of ring origin by this process makes it hard to assess how restrictive it would be compared to other contemporary ring origin ideas. The viability of a condensation model would appear to depend on the nature of satellite accretion, the assumed lifetime and thermal evolution of the protosatellite disk, and considerations involving the timing and rate of gas inflow to the disk (also see discussion in section 18.3.3.6 below). Although these issues are (and will remain) uncertain, progress could be made by using traditional assumptions as a starting point to evaluate the feasibility of ring origin via condensation compared to other ideas that also, by necessity, rely on such assumptions.

### 18.3.3.2 Tidal Disruption of a Small Moon

In 1847, Edouard Roche suggested that Saturn’s rings originated when a small moon strayed within the Roche limit and was torn apart by tidal forces (Roche, 1849). While appealing in its simplicity, this idea has generally been disfavored of late due to the perceived difficulty in effectively disrupting a Mimas-sized object. Tidal stresses on a density  $\rho$ , radius  $R$  satellite with semi-major axis  $a$  and orbital frequency  $\Omega$  are of order  $T \sim \rho \Omega^2 R^2$  (e.g., Weidenschilling et al., 1984). For small objects, material strength inhibits tidal disruption, while for larger objects, self-gravity dominates and strength is less important. The transition between these two regimes occurs at  $R \sim 200$  km for solid ice (Sridhar and Tremaine, 1992), which is approximately the size of a progenitor moon whose mass is comparable to that in the current rings.

In the limit of no strength and a fluid-like, self-gravitating body, the relevant tidal disruption distance would be the classical Roche limit (Eq. 18.2). However, a small, Mimas-sized ring progenitor would likely need to orbit well within the Roche limit to disrupt, probably interior to the inner edge of the current main rings (Jeffreys (1947); Aggarwal and Oberbeck (1974); Davidsson (1999); also see section 4.2.2 in Charnoz et al. (2009b)), and perhaps even interior to the expected early position of Saturn’s surface (see figure 18.4 below). If the ring progenitor was a regular moon, it would need to evolve from an orbit substantially outside its Roche limit (where it could have initially formed) to one well within the Roche limit. If this were accomplished through interactions with a gas disk, the resulting dispersed fragments would be vulnerable to loss via gas drag, because gas densities high enough to drive a small moon’s inward migration through gas drag would cause a much faster destruction of its mass when spread amongst small fragments. Finally,

complete disruption of a nominal composition satellite that contained rock and ice in roughly solar proportions would lead to a rock-ice ring, rather than a nearly pure ice ring. Thus a tidal disruption model needs to be considered in conjunction with a model for producing an extremely rock-poor icy progenitor moon.

### 18.3.3.3 Collisional Disruption of a Small Moon

Another ring origin theory proposes that during the satellite formation era, a  $\sim 200$  km radius, few  $\times 10^{22}$  g satellite drifted inward to an orbit interior to its Roche limit, located at  $r_R = 2.45R_S(\rho_p/\rho)^{1/3} \approx 2.17(\rho/1 \text{ g cm}^{-3})^{-1/3}R_S$ . In this classic expression,  $R_S$  is Saturn's mean radius rather than its equatorial radius, with  $R_S = 58,232$  km currently. The satellite remains interior to the Roche limit until a later time when it is disrupted by a heliocentric impactor (e.g., Harris, 1984; Charnoz et al., 2009a,b). The collisional disruption model addresses two key deficiencies of the tidal disruption model. First, hydrocode simulations (e.g., Benz and Asphaug, 1999) show that a high-velocity cometary impactor of radius 10 to 20 km could disrupt a 200-km radius moon in the region of the main rings, with the resulting fragments prevented from re-accumulation by planetary tides. Second, although interactions with a gas disk are likely needed to bring the moon to within the Roche limit, the event leading to the creation of the ring can be delayed until a much later time when the gas disk had dissipated, removing the vulnerability of the ring to loss via gas drag.

The disruption of a ring progenitor moon requires a large number of potential cometary impactors to be probable. Estimates of the current population of such objects are too low by at least an order of magnitude to make such an event likely in the past billion years (e.g. Charnoz et al., 2009a). However, the number of outer Solar System impactors could have been much larger in the distant past. Charnoz et al. (2009a) considered the Late Heavy Bombardment (LHB) predicted by the so-called Nice model for the origin of the structure of the outer Solar System. They estimated near-certain disruption of a hypothetical  $\sim 200$ – $300$  km radius progenitor moon during this period, predicted to occur some 400 Myr to 1 Gyr after the planets formed. In the Nice model, the enhanced bombardment is driven by the destabilization of a background planetesimal disk of comets as Jupiter and Saturn cross a mutual mean-motion resonance and the orbits of the ice giants are scattered outward (see Dones et al., 2015, for a review of the history of the cometary reservoirs, including a discussion of the Nice model and its successors). In general, the structure of the Kuiper Belt requires that Neptune migrated outward via planetesimal scattering (e.g., Malhotra, 1995), and this implies both an initially more compact giant planet configuration and a planetesimal disk containing between 10 and 100 Earth masses (e.g., Fernandez and Ip, 1984; Hahn and Malhotra, 1999). The interaction of the giant planets with such a massive disk would appear likely to produce an early enhanced bombardment period even if the details of the evolution differed from those of the Nice model. Thus the disruption of

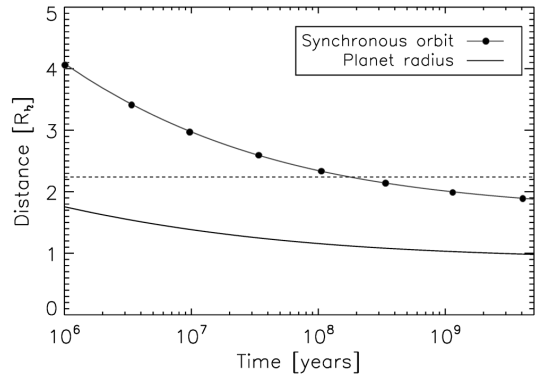


**Figure 18.4** Estimates for Saturn's radius (solid line) and the location of synchronous orbit (dotted solid line) for the first billion years of the planet's history (Salmon and Canup, 2016). The dashed line shows the approximate Roche limit for ice.

a Mimas-sized moon orbiting within the Roche limit – if one existed – seems probable during this period.

Maintaining a ring progenitor moon interior to the Roche limit until the time of the LHB places constraints on both the moon's mass and the early tidal parameters for Saturn. A moon exterior (interior) to the synchronous orbit at Saturn migrates outward (inward) due to interaction with tides it raises on the planet. For Saturn's current rotation rate, the synchronous radius is located at 112,000 km, or at  $a_{sync} \approx 1.92R_S$ . However, for the first billion years of its history, Saturn would have been larger than its current size (e.g., Fortney et al., 2007). By conservation of spin angular momentum, Saturn would have then rotated more slowly, with  $a_{sync}$  initially well exterior to its current location, evolving inward to the Roche limit after  $\sim 10^8$  yr and to near its current location in  $\sim 10^9$  yr (Canup, 2010; Salmon and Canup, 2016, and figure 18.4).

A primordial ring progenitor moon that drifted inside the Roche limit (e.g., via gas drag) would undergo inward tidal evolution, with rate

$$\frac{da}{dt} \sim \left(\frac{3k_2}{Q_p}\right) \left(\frac{GM_p}{R_p}\right)^{1/2} \left(\frac{M}{M_p}\right) \left(\frac{a}{R_p}\right)^{-11/2}, \quad (18.8)$$

where  $k_2$  and  $Q_p$  are the tidal Love number and dissipation factor for the planet, and  $R_p$  is the early planet's radius (as distinct from  $R_S$ , Saturn's current mean radius). The timescale for a primordial moon of mass  $M$  to evolve tidally inward from the Roche limit to the planet's surface is

$$\begin{aligned} \Delta t &\sim \frac{(r_R/R_p)^{13/2}}{20(k_2/Q_p)(M/M_p)(GM_p/R_p^3)^{1/2}} \\ &\sim 10^9 \text{ yr} \left(\frac{3 \times 10^{-6}}{k_2/Q_p}\right) \left(\frac{5 \times 10^{22} \text{ g}}{M}\right) \left(\frac{1.1R_S}{R_p}\right)^5 \end{aligned} \quad (18.9)$$

where the second line considers an icy moon with density  $\approx 1 \text{ g cm}^{-3}$  so that  $r_R \approx 2.2R_S$ , a somewhat enlarged planet with  $R_p = 1.1R_S$  (this quantity would actually be time-dependent as the satellite evolved, as in figure 18.4), and  $k_2/Q_p = 3 \times 10^{-6}$  for, e.g.,  $k_2 = 0.3$  and  $Q_p = 10^5$ . Thus for a primordial moon to survive within the Roche limit until the time of the LHB requires both that the early



$Q_p$  for Saturn was large (i.e.,  $\geq 3 \times 10^4$  for  $k_2 = 0.3$ ; e.g., Charnoz et al., 2009b) and that the moon was small, similar in mass to the current rings. In contrast, a moon that was, e.g.,  $10^2$  times more massive than the current rings would decay into Saturn in  $\leq \text{few} \times 10^7$  yr, even assuming a large  $Q_p = 10^5$  (i.e., slow tidal evolution). Similarly, even a small moon with a mass a few  $\times 10^{22}$  g would be lost if very rapid tidal evolution applied to the early Saturn (i.e., with  $Q_p \sim 10^3$ , as has been advocated by some recent works: Lainey et al., 2012; Charnoz et al., 2011; Lainey et al., 2017).

Assuming that an appropriate satellite could be delivered to and maintained within the Roche-interior region until the time of the LHB, a remaining question for the collisional disruption theory is that disruption of a nominal rock-ice satellite would produce an initial rock-ice ring, rather than a pure ice ring. One possibility is that the rock might be preferentially removed from the ring if it were initially contained in much larger intact fragments that migrated relative to the ice due to ring-moon interactions (Charnoz et al., 2011, also see section 18.3.3.7 below). Alternatively, disruption of an essentially pure ice progenitor moon would produce a pure ice ring, but this then requires an explanation for the origin of such an object.

#### 18.3.3.4 Tidal Disruption of a Comet Interloper

Dones (1991) proposed that Saturn’s rings originated when a heliocentrically orbiting Centaur (comet) of radius  $\sim 200$  to 300 km passed well within Saturn’s Roche limit and was tidally disrupted. For an initially intact object on a parabolic encounter with the planet, the inner portions of the object facing the planet upon disruption will have a velocity somewhat less than the local escape velocity from Saturn, and so will be weakly bound to the planet. The percentage of the interloper’s mass that can be “disintegratively captured” increases with the size of the interloper and with decreasing periape distance, reaching a maximum theoretical value of 50% (Dones, 1991; Charnoz et al., 2009b). Disintegrative capture of a rubble pile that was an intimate mixture of ice and rock would produce a rock-ice ring. However, if the object was instead differentiated into a rock core and an icy mantle, the bound debris could be overwhelmingly icy (Dones, 1991). This has been numerically confirmed in recent SPH simulations in the case of a Titan-sized object, as we describe in the next section (Hyodo et al., 2017). A differentiated state would be expected if substantial melting of the comet’s ice had occurred (e.g., Barr and Canup, 2010), suggestive of an intact object with substantial strength. How the inclusion of strength might modify the disruptive capture process for comets comparable in mass to the current rings is not clear; it would be unimportant for objects that were much more massive.

Initially, captured debris would be on highly eccentric orbits with semi-major axes of hundreds of saturnian radii (Hyodo et al., 2017). In the absence of other processes, dissipative collisions between debris particles would circularize their orbits while approximately conserving angular momentum, leading to a ring interior to the Roche limit (Dones, 1991). However, initial debris orbits would cross those of the

regular Saturnian satellites. As such, the efficiency of ring production would be a function of the rate of mutual debris collisions compared to the rate of debris sweep-up by the satellites. This process has not been modeled.

For the current cometary flux, close passages by large comets appear unlikely in the age of the Solar System (Dones, 1991). During an outer Solar System LHB, such encounters would have been common, although Saturn proves to be the giant planet least likely to have experienced such an event (Charnoz et al., 2009a,b). This is due to several factors, including Saturn’s low density, which makes the region over which comet encounters lead to captured material smaller than those of the other giant planets, which have higher densities (Asphaug and Benz, 1996). Jupiter, Uranus and Neptune are estimated to each receive about an order of magnitude more mass through close comet encounters than does Saturn (Charnoz et al., 2009b, their fig. 5). Thus, if Saturn’s rings originated by disintegrative capture, one would expect the other planets to have ring systems at least as massive as Saturn’s too. The lack of such systems suggests that while close passages of comets may have been common in the early Solar System, their debris did not typically produce long-lived rings, due to, e.g., escape of high-eccentricity tidal debris from planetary orbit and/or efficient sweep-up of debris by satellites (e.g. Charnoz et al., 2009b). An alternative solution would be that for some reason, the rings of Uranus and Neptune are short-lived while those of Saturn are long-lived. However, why there would be such a difference between the lifetime of rings of the different planets is not understood. This remains an open question.

#### 18.3.3.5 Recent Developments: The possibility of a super-massive primordial ring at Saturn

While the mass of Saturn’s current rings is many orders of magnitude larger than that of the other ring systems, it still represents in total only a small, several hundred km-sized moon. The origin models described above were designed to produce an initial ring whose mass is comparable to that in Saturn’s current rings,  $\sim \text{few} \times 10^{22}$  g. However, recent developments suggest that the current ring mass may not actually reflect the initial ring mass. As described in section 18.2, the viscosity in a massive ring is proportional to its mass squared, so that a very massive ring spreads rapidly, causing its mass to decrease and its spreading rate to slow until the spreading timescale becomes comparable to the age of the system. Simulations of the viscous evolution of a ring at Saturn have shown that the current ring mass is comparable to that achieved as a more massive initial ring viscously evolves over 4.5 billion years (figure 18.1; Salmon et al., 2010), independent of the starting ring mass. This agreement could, of course, be coincidental. However, perhaps a more compelling interpretation is that the mass of Saturn’s current rings reflects their dynamical age, which could be billions of years. Other data would be necessary to unambiguously infer the rings’ using radiogenic dating techniques. Ideally a sample return mission from Saturn’s rings would be the best, but does not seem within reach of current technologies. The primordial progenitor of Saturn’s ring

system then could have been much more massive and still, after billions of years of collisional evolution, have left a ring comparable in mass to that seen today.

How could such an initially massive ring have formed? Based on the arguments above, formation by collisional disruption of a pre-existing satellite does not appear likely, as it would be extremely improbable in the short time a large moon would spend inside the Roche limit before tidally evolving into the planet. For example, per Eq. (18.9), a  $10^{25}$  g satellite would tidally decay from the Roche limit to Saturn’s surface in only a few million years even for large  $Q_p$ .

In contrast, tidal disruption could produce a massive ring if the interloper was massive, in a scaled-up version of the Dones (1991) model. This possibility has been recently considered by Hyodo et al. (2017), who consider tidal disruption of a single hypothetical differentiated Titan-sized passing Kuiper Belt Object.<sup>3</sup> Charnoz et al. (2009a) predict that close passes by  $500 \text{ km} \leq R \leq 2000 \text{ km}$  objects would be rare events even during the LHB, but the probability of such an event depends sensitively on the size distribution of large objects at that time, which is uncertain. Using hydrodynamical simulations, Hyodo et al. (2017) find that a differentiated Titan-sized object passing as close as 3 planetary radii may have its icy mantle shattered by tides, producing an ice-rich debris disk whose mass is compatible with the formation of Saturn’s current rings, as well some or all of Saturn’s inner moons (see section 18.3.3.7 below). The silicate-rich core, as well as most of the incoming object’s mass, go onto hyperbolic orbits and are lost from the planet. However, a very small portion of the silicates (a fraction of a percent) may also be captured and may contribute to the current silicate content of the moons. An appealing aspect of this scenario is that it can produce an ice-dominated ring at Saturn with little silicates. However, tidal disruption in general would be equally likely to produce a prograde or a retrograde ring, as the final debris would orbit in the same direction as the passing body. But clearly a single prograde system like that at Saturn would result half the time.

A more challenging issue is that a size distribution of background objects consistent with such an event at Saturn would imply that the other outer planets would have had massive rings produced by tidal disruption too, as discussed in the prior section and in Charnoz et al. (2009a). Such rings would have viscously evolved to an asymptotic state whose mass is many orders of magnitude larger than those of the other very low-mass ring systems, per the arguments in section 18.2.2 and in figure 18.1. An additional process would then be needed to remove such early massive rings at the other giant planets but not at Saturn. It is not clear what could accomplish this. Processes associated with the Sun’s radiation can remove small particles through inward orbital decay, but these would be substantially weaker at Uranus and Neptune than at Saturn for a given parti-

<sup>3</sup> No KBOs of this size have yet been discovered. The most massive Kuiper Belt Object known, Eris, has a mass 12% that of Titan. However, much more massive KBOs may have been present in the early Solar System and may yet exist in the distant Kuiper Belt or inner Oort Cloud.

cle size. We return to the interesting issue of potential early massive rings at Uranus and Neptune in section 18.4.2.

Alternatively, a massive ring could be produced through tidal disruption if a massive satellite migrated interior to the Roche limit. It has long been recognized that interaction with a primordial gas-rich disk around Saturn would cause small moons to spiral inward due to aerodynamic gas drag (e.g., Harris, 1984). The migration rate due to this process is inversely proportional to the moon’s physical radius, and is thus not important for large moons on relevant timescales. More recent work has focused on the ability of density wave interactions with a gas disk to modify the orbits of large satellites (e.g., Canup and Ward, 2002; Mosqueira and Estrada, 2003a,b). Such interactions can cause a satellite’s orbit to spiral inward with a rate that is proportional to the satellite’s mass (Type I migration; Ward, 1986), or, for even larger satellites capable of opening gaps in the gas disk, the satellite’s orbital motion becomes coupled to the local viscous expansion of the disk (Type II migration; Lin and Papaloizou, 1986). The survival of Titan and galilean-sized moons against such potentially destructive processes has provided new constraints on satellite formation conditions and motivated the development of new satellite origin models (e.g. Canup and Ward, 2002; Mosqueira and Estrada, 2003a,b; Alibert et al., 2005).

An aspect on which all models do not agree, and that is still an open question, is the delivery of solids to the circumplanetary disk. Indeed, as grains grow and progressively decouple from the gas in the outer Solar System, it is increasingly difficult for them to penetrate a planet’s circumplanetary disk due to the pressure gradient created by the planet in its surroundings. While Canup and Ward (2002) consider that grains are small and are transported with the gas, in Mosqueira and Estrada (2003a,b) and Alibert et al. (2005), grains are considered to be big and decoupled. They are scattered in the disk by nearby planets. Recent works modeling “pebble accretion” advocate an essentially bi-modal planetesimal population in which small pebbles are accompanied by  $> 100$ -km planetesimals formed via gravitational instability (e.g., Levison et al. (2015)), which could imply a larger population of small, gas-coupled objects than assumed by prior works that consider power-law planetesimal size distributions. Overall, the mechanism of solid delivery remains an open and important question, which depends strongly on the relative timing of grain growth and giant planet growth in the outer Solar System.

While models for the formation of outer planet satellites vary, a general implication of density wave interactions is that they provide a means for much more massive satellites to migrate inward to the Roche-interior region, where they might then become a source for ring material.

Perhaps the most explored model to date is one in which regular satellites form within a disk supplied by an ongoing inflow of gas and solids from heliocentric orbit as a gas planet completes its growth (Canup and Ward, 2002, 2006; Alibert et al., 2005; Ward and Canup, 2010; Sasaki et al., 2010; Ogihara and Ida, 2012). These models are based on the recognition that the period over which inflow to the disk occurs may be long, comparable to the lifetime of the solar

nebula ( $\geq 10^6$  yr), so that satellites may accrete during the inflow phase, rather than after it, as assumed by prior models.

In an actively-supplied disk, the gas component likely reflects a quasi-steady state between the inflow supply and viscous spreading, so that as the nebula dissipates and the inflow slows, the disk becomes increasingly “gas-starved”. Solids flowing into the disk provide the source material for growing satellites, while Type I interaction with the gas disk cause each satellite’s orbit to spiral inward at a rate proportional to its growing mass. The balance of these two processes causes there to be a critical maximum mass for a satellite of a gas giant planet, which for reasonable disk and inflow parameters is comparable to the mass of Titan at Saturn, and the mass of the galilean satellites at Jupiter (Canup and Ward, 2006). Each satellite grows no larger than this critical mass before it spirals inward into the planet. As satellites are lost, new ones grow in their place as more solids flow into the disk. Multiple generations of large satellites form and are lost, each having a similar mass compared to that of the host planet, with the satellite system mass oscillating about a quasi-steady-state value of  $10^{-4}$  planet masses, independent of the total mass processed through the disk (Canup and Ward, 2006). This value is comparable to the satellite system mass ratios observed around all the outer planets. The overall process continues until the inflow itself ends and the last system of satellites stabilizes as the gas disk dissipates and Type I migration ends (Canup and Ward, 2002, 2006; Sasaki et al., 2010; Ogihara and Ida, 2012). Galilean-like systems with multiple large satellites are the most common outcome seen in direct  $N$ -body simulations of this process (Canup and Ward, 2006; Ogihara and Ida, 2012), but systems with one large Titan-like satellite are possible if inner large satellites migrate inward and are lost as inflow to the planet ends (Canup and Ward, 2006; Canup, 2010, her Fig. 1).

Other works consider that the satellites formed after the inflow to the disk ended, so that the disk has a constant total mass, and envision a very low-viscosity disk so that large satellites may open gaps and halt their orbital migration (Mosqueira and Estrada, 2003a,b). In this case, satellite survival is predicted for satellites that exceed a critical gap-opening mass, implying that satellites of this mass or greater may survive. For an inviscid disk, the gap-opening mass can be comparable to the mass of Titan and the Galilean satellites (Mosqueira and Estrada, 2003a,b), and for this case the constant-mass disk model predicts a minimum satellite system mass ratio of order  $10^{-4}$  planet masses. However, in this model, there is not a limit on how much larger than the gap-opening mass satellites may grow, and instead, the final mass of the satellites is a function of the assumed initial disk mass. This conceptually distinguishes the constant-mass disk models from the actively-supplied disk models, because in the former the final satellite system mass depends on the assumed mass of the initial disk (which is highly uncertain), while the latter predict a common satellite system mass ratio independent of the mass processed through the disk.

In both the actively-supplied disk and constant-mass disk models, inward migration of satellites to within the Roche limit may occur due to density wave interactions with the gas disk. In the inflow-supplied disk models, Type I migration leads to repeated losses of Titan-sized objects at Saturn. Smaller inner satellites might evolve inward due to tides, but satellites migrate inward over large distances due to density wave interactions only once they reach very large, Titan-like masses (Canup and Ward, 2006). In constant-mass, inviscid disk models, large satellites would be protected from migration by opening gaps, while smaller satellites might migrate inward due to Type I migration and be lost. The latter merits further consideration by direct models of satellite accretion within such disks to determine the properties of potential ring progenitors.

### 18.3.3.6 Tidal Stripping from a Large Satellite

The developments above – in particular, the prediction that one or more Titan-sized satellites at Saturn migrated into the planet at the end of the satellite formation era – motivated a new model for ring origin, in which a massive primordial ring is formed as tides strip the icy outer layers from a large satellite as it spirals into Saturn (Canup, 2010).

For a gravity-dominated, Titan-sized satellite, tides will begin to remove mass once the satellite’s orbit migrates within the Roche limit set by its mean density, which is located at  $\approx 1.75 R_S$  for a Titan-density satellite. The nature of the resulting mass loss depends on the satellite’s interior structure. An undifferentiated, uniform composition satellite would disrupt completely. However, a Titan-sized moon would be expected to have a differentiated interior, with an ice mantle overlying a rocky core, due both to the energy of its accretion and strong tidal heating as its orbit spiraled toward the planet; see detailed calculations and estimates in Barr and Canup (2010) and Canup (2010). For a differentiated ice-rock satellite, tides will first remove material from its outer ice shell. The preferential removal of ice then causes the satellite’s mean density to increase slightly until the remnant satellite is marginally stable at its current distance (Canup, 2010). Continued inward migration (due to, e.g., Type I migration and tidal interaction with Saturn) would then lead to additional ice removal, with the process continuing until either the remnant satellite collides with the planet or its higher-density rocky core disrupts (Canup, 2010). The Roche limit for rock of density  $\rho_{\text{rock}}$  is at  $r_{R,\text{rock}} = 1.5 R_S (3 \text{ g cm}^{-3} / \rho_{\text{rock}})^{1/3}$ . Planet contraction models predict that Saturn’s early radius would have been between  $R_p = 1.5 R_S$  and  $R_p = 1.7 R_S$  (Marley et al., 2007; Fortney et al., 2007, see also figure 18.4 above). For  $r_{R,\text{rock}} \leq R_p$ , the remnant satellite would collide with the planet before its rocky core disrupts. In this case tidal stripping would produce an essentially pure ice ring. The silicates of today’s satellites may have been provided by a tiny fraction of silicates stripped from the initial Titan-sized progenitor (see Charnoz et al., 2011, and section 18.3.3.7).

Figure 18.5 shows a hydrodynamical simulation to simulate tidal stripping from a differentiated Titan-sized satellite as it spirals inward from its initial Roche limit (Canup,

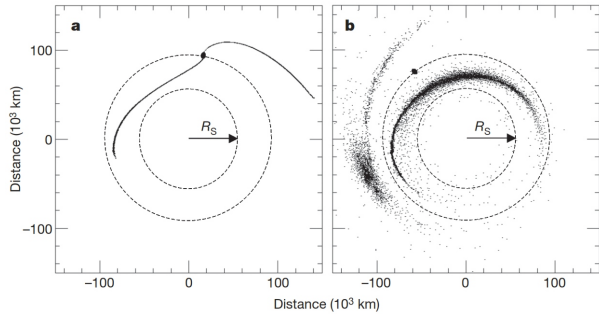


**Figure 18.5** SPH simulation showing the tidal removal of ice from a differentiated, Titan-mass satellite, from Canup (2010). Type I migration and tidal interaction with the planet cause the satellite's orbit to spiral inward from its initial Roche limit ( $a_{max}$ ) to the planet's surface ( $R_p$ ) in  $\sim 10^4$  yr. The satellite's evolution across this region is tracked with a series of SPH simulations that treat the satellite and planet explicitly but do not include the gas disk. The satellite starts with  $a = a_{max}$  and is evolved for several orbits with SPH to simulate tidal mass removal and the establishment of a stable satellite remnant. The remnant satellite is then shifted inward by  $\Delta a \sim 10^{-2}a$  and re-simulated, with the process repeated until  $a$  is small enough that the satellite's rocky core disrupts, which determines the minimum planetary radius consistent with the creation of a pure ice ring. Frames here show tidal stripping from a 50% ice, 50% rock satellite at  $a = 0.97a_{max}$  after 8 simulated hours [a] and 25 hours [b]. Distances are shown in units of  $10^3$  km; for comparison, Saturn's B and A rings lie between  $\sim 92,000$  and  $137,000$  km. Dashed circles indicate the satellite's orbit and Saturn's current mean radius,  $R_S$ ; Saturn's radius at the time of the satellite's decay was likely  $R_p \geq 1.5R_S$  (e.g., figure 18.4).

2010). Material originating from the satellite's ice mantle is lost through its inner and outer Lagrange points ( $L_1$  and  $L_2$ ), leading to particles on eccentric orbits (with  $e \sim 10^{-1}$ ) with semi-major axes interior and exterior to that of the satellite, respectively. Subsequent collisions between particles will tend to circularize their orbits. Interior particles may collide directly with the planet or be driven into the planet by the satellite as it continues to migrate inward, while exterior particles can supply the eventual ring. The total mass of ice produced via tidal stripping depends on the satellite mass and the location of the planet's surface at the time of the satellite's demise. For a Titan-sized body, in the limit that  $a_{R,rock} = R_p$ ,  $\sim 10^{25}$  g of ice is stripped into orbits exterior to the satellite for a Titan-sized body ( $\sim 10\%$  of the original satellite's mass), while if  $a_{R,rock} < R_p$ , less ice is produced before the remnant satellite hits the planet (Canup, 2010).

As each ringlet of ice is stripped, strong shepherding torques from the remnant satellite rapidly repel it, driving exterior material into orbits beyond the Roche limit for ice in  $\sim 10^2$  yr. Once this material orbits substantially beyond its Roche limit (e.g.  $> 1.1r_{R,ice}$ ; Canup and Esposito, 1995, 1996) it can rapidly accumulate, forming a pure ice moon whose final mass is  $m_o \leq 10^{25}$  g. The ice stripped from the progenitor satellite is then stored for a time in this secondary moon, which on a longer timescale (because its mass is substantially smaller than the original Titan-sized progenitor)

spirals back inward due to tidal interaction with Saturn. The ice moon takes  $\sim 10^6$  yr  $[3 \times 10^{-6}/(k_2/Q_p)] [10^{25}g/m_o]$  to tidally decay back within the Roche limit, where it disrupts into a massive ice ring (Canup, 2010). This expression considers a small value for  $k_2/Q$  for primordial Saturn, based on traditional estimates (e.g., Goldreich and Soter (1966)). This is not necessarily inconsistent with much more rapid tides observed today (e.g., Lainey et al. (2012, 2017)), as recent work proposes that the current values reflect resonance locking between moons and internal oscillation modes in the planet, a process that implies larger effective  $Q$  values in the past (Fuller et al., 2016). We return to this issue in section 18.3.3.9.

Because the tidal stripping model relies on interaction with the gas disk (e.g., Type I migration) to deliver the ring progenitor to the Roche interior region, the potential vulnerability of the ring to loss via gas drag must be considered (Canup, 2010). Consider a gas inflow to Saturn that decays exponentially with time with a time constant  $\tau_g \sim 10^6$  yr, reflecting a waning inflow to the disk due to the dispersal of the solar nebula. That Titan survived while a similarly massive interior satellite was lost implies that Titan's timescale for Type I decay was comparable to  $\tau_g$ , implying a very low  $\Sigma_g \sim \text{few to } 10 \text{ g cm}^{-2}$  at the time the last large inner satellite was lost (Canup, 2010). The gas density would decrease further in the  $\sim 10^6$  yr required for the secondary moon to tidally decay inward and be disrupted.

Thus a ring produced by tidal stripping can survive gas drag until after the gas disk has dissipated, so long as the progenitor satellite migrates within the Roche limit near the very end of the gas disk lifetime. Survival of the ring thus does require special timing: the actively-supplied disk models show that many large satellites were likely lost to inward migration, and the rings produced by nearly all of them would have been lost to gas drag. But at some point we know that the gas disk around the planet dissipated and the loss of large satellites via inward migration must have ended. The key question is then: what was the fate of the last ring created by such a process? For Saturn, the lack of a large inner companion to Titan (one of the most challenging features to explain in the Saturnian system) may imply the very late orbital decay of the inner body, and this implies conditions favorable for ring survival as described in the prior paragraph. However even the final episode of tidal stripping could have been unsuccessful in producing a long-lived ring in other circumstances. For example in the context of the actively-supplied disk models, Jupiter, in contrast to Saturn, must have retained its final generation of large interior satellites (i.e., Io and Europa) as inflow to that planet ended. One expects that Jupiter would still have lost large interior satellites from prior generations of moons that formed when the gas inflow rate to the planet was higher and the disk was more gas-rich (Canup and Ward, 2002, 2006). Jupiter's final ring produced by tidal stripping would have likely been lost to stronger gas drag. Thus tidal stripping offers a mechanism that would frequently have produced rings as large satellites migrated within the Roche limit, but only the final such rings could survive, and even then not in all circum-

stances. This offers an appealing explanation for why Saturn alone has a massive ring today.

An overall strength of the tidal stripping model is that it would naturally produce an essentially pure ice, prograde ring. While the model was developed under the premise of a particular model of satellite formation (Canup and Ward, 2002, 2006), it could apply to other situations and other models as well. The basic requirements for the production of a long-lived ring via tidal stripping model are (1) a differentiated rock-ice satellite that orbitally migrates within the Roche limit, and (2) a ring decay timescale due to gas drag (Eq. 18.7) that exceeds the lifetime of the gas disk. The case for a differentiated ice-rock satellite is strongest for a very large satellite because of its substantial accretional and tidal heating, which would generally imply a massive ring even if other aspects of the evolution or the satellite accretion model differed.

An important overall caveat to the tidal stripping model is that it considers ring formation as a byproduct of satellite formation, a broad topic which itself remains quite uncertain. Multiple key general uncertainties persist in our understanding of the protosatellite environment, including the radial and temporal structure of the circumplanetary disk, the time variation of the inflow of gas to such a disk, the presence or not of viscosity and the accretion rate onto the planet, the delivery of solids to the disk and their accretion within the disk, and the role that the magnetic field may or may not play in providing turbulence. Substantial progress may result from future hydrodynamical simulations of giant planet growth that simultaneously consider inflowing material, as well as the accompanying disk and planet structure, although it is clear that such models are still challenging for even high-performance simulations and will likely be for years to come. It may also be possible to apply recent advances in planetesimal formation made in the context of planet accretion (e.g., Levison et al. (2015) and references therein) to make better progress in understanding satellite growth as well. Improved knowledge of these many processes will be necessary to better evaluate our models of satellite formation, as well as the ring origin models linked to the satellite formation environment, including the condensation and tidal stripping models.

### 18.3.3.7 Implications of a Massive Initial Ring

A massive primordial Saturnian ring requires an explanation for what happened to perhaps  $\sim 99\%$  of the ring material as it evolved over 4.5 billion years. As a ring viscously spreads, ring material is depleted both by collision onto Saturn at the ring's inner edge, and by spreading of material beyond the Roche limit at the ring's outer edge. Once ring material is substantially outside the Roche limit, ring material can accrete into satellites. Spawned moons evolve outward, due, at first, to resonant interactions with the ring and then by tidal evolution, with the mass of spawned moons decreasing with time as the mass of the ring decreases due to viscous spreading (Crida and Charnoz, 2012). This process was first directly simulated for a ring similar in mass to Saturn's current rings by Charnoz et al. (2010), who demonstrated that

the very small innermost Saturnian moons (out to and including Janus) were likely spawned from the rings in the recent past. However, it was clear based on that work that a more massive ring would give rise to more massive moons as it viscously evolved.

Canup (2010) estimated that a massive ring produced via tidal stripping from a Titan-sized satellite would have a total mass and angular momentum consistent with the current rings and the inner Saturnian moons out to and including Tethys ( $\approx 5R_S$ ), and that the first spawned satellite from such a ring would have a mass comparable to that of Tethys ( $\approx 16\times$  the mass of Mimas). These expectations have generally been confirmed by numerical simulations (Charnoz et al., 2011; Salmon and Canup, 2015). However, the final orbital architecture of the satellite system spawned from a massive ring depends on the assumed value of the tidal parameters for Saturn. Estimates of the time-averaged tidal parameter for Saturn have traditionally been in the range  $10^{-6} \leq k_2/Q_p \leq 10^{-5}$  (Goldreich and Soter, 1966), which implies that the moons out to Tethys (or their progenitors, since the inner moons may have been disrupted and re-accreted (Charnoz et al., 2009b)) were spawned from the rings (Salmon and Canup, 2015). This offers an appealing explanation for the unusually ice-rich composition of these inner moons, which, as a group, are about 90% ice by mass. Tethys in particular is the most ice-rich satellite larger than 100 km in radius known in the Solar System, containing  $\leq 6\%$  rock by mass. In contrast, the large Uranian satellites contain about half rock, and even low-density Miranda contains about 20% rock. However, Enceladus is currently about half rock, and if it or its progenitor were spawned from an icy ring, this rock would need to have been somehow supplied by external sources. One possibility is that later impacts delivered rock to these moons. Indeed, the estimated rock delivered to the inner Saturnian moons during the LHB is roughly comparable to their current total rock content (Canup, 2013; Salmon and Canup, 2014). However, whether external bombardment alone can explain the current distribution and variation of densities for the inner moons is not clear, and remains an outstanding issue for such models. Alternatively, there may have been a small portion of rock in the initial ring due to, e.g., tidal stripping from an incompletely differentiated satellite, or tidal disruption of a large body that leaves some portion of the object's silicates in orbit as well.

Satellites spawned from a massive ring would have achieved orbits well beyond that of Tethys if the outward tidal evolution of satellites had been much more rapid. Recent astrometric results imply  $Q_p \sim 10^3$ , or  $10^{-4} \leq k_2/Q_p \leq 10^{-3}$  for the current Saturn system (Lainey et al., 2012, 2017). The evolution of a massive ring and its spawned moons was independently simulated in Charnoz et al. (2011), who considered rapid tidal evolution, with  $k_2/Q_p \sim 10^{-4}$  motivated by these results. For such rapid tides, a massive ring could spawn not only the inner Saturnian satellites, but objects as distant and massive as Dione and Rhea as well (see also Crida and Charnoz, 2012). Dione and Rhea contain  $\sim 10^{24}$  g in rock, much more than the total rock in the inner moons ( $\sim 10^{23}$  g). Charnoz et al.

(2011) argued that Saturn’s initial ring had a substantial rock component, with the rock initially in the form of large chunks that were able to open gaps in the ring and undergo Type II migration, so that the ring’s rock was preferentially removed. Using a direct simulation of a Rhea-sized rocky chunk embedded in a ring, they showed that the chunk is expelled from the ring’s outer edge, where it could then form the core of a spawned satellite. They suggested that stochastic variation in such a process could explain the varied densities of the inner saturnian moons. Whether this rock removal process would be efficient enough to yield a nearly pure ice ring for a realistic initial size distribution of rock fragments is not clear. Further, the Lainey et al. (2012) determination of  $Q_p \sim 10^3$  for Saturn, while intriguing, remains controversial because it implies a much different  $Q_p$  for Saturn than similar techniques indicated for Jupiter (Lainey et al., 2009). However, a recent re-evaluation of  $Q_p$  based on astrometric data and using Cassini images was independently obtained by two teams (IMCCE in Paris and JPL in USA) using different tools. Both teams agree that  $Q_p$  is indeed very small, so that Saturn’s tides appear strong, at least for the current system (Lainey et al., 2017). Whether this low value has applied to Saturn over its entire history is not known.

Thus substantial progress has been made on the possible formation of a massive ice ring at Saturn as the precursor to the current rings. However, there remain important open issues concerning whether and how such a ring could evolve into the system of rings and moons we see today.

### 18.3.3.8 Pollution of an Early-Formed Saturnian Ring

Explaining how Saturn’s rings remain so rock-poor today presents an ongoing challenge to all of the origin models we have discussed, which invoke either a primordial origin, or an origin some 1 Gyr later during the LHB. Thus all imply a ring age of several billion years. Even if one begins with a pure ice ring, prior estimates suggest that the ring would excessively darken over  $\sim 10^9$  yr. To avoid this, the pollution rate due to micrometeoroid bombardment estimated previously (e.g., Cuzzi and Estrada, 1998) must be too rapid, due to either an underestimation of the rings’ total mass or to an overestimation of the bombardment rate, or both (e.g., Cuzzi et al., 2010). In addition, some Cassini observations and  $N$ -body simulations have been interpreted to suggest that the B ring contains substantially more mass than Voyager-era estimates (Robbins et al., 2010), implying a higher likelihood that the rings are primordial, although others infer a total mass similar to prior estimates (e.g. Refet et al., 2015) or somewhat lower (Hedman and Nicholson, 2016). Whereas all estimates are about the same order of magnitude, better constraints are expected from the end of the Cassini mission, in particular from the first direct measurement of the total ring mass as the spacecraft undergoes close passes to the rings prior to its descent into Saturn.

### 18.3.3.9 A model for making young rings : resonant collisions in the satellite system

Ćuk et al. (2016) propose that recent collisions between icy moons could provide a viable mechanism to form today’s rings. Their argument is two-fold, and is based on the recent measurements of Saturn’s tidal dissipation, the so-called  $Q_p$  parameter present in Eq. (18.8), by Lainey et al. (2017). The recently determined value of  $Q_p$  implies intense tidal dissipation inside Saturn and is consistent with the heat flux at the surface of Enceladus. As a consequence, Saturn’s satellites may undergo a rapid tidal evolution of their orbits. If Saturn’s satellite system was as old as Saturn itself, then this would imply that Tethys and Dione may have crossed their mutual 3:2 resonance in the recent past (about 100 Myr ago). During this resonant configuration, both orbits become significantly eccentric and inclined. While the eccentricities can damp due to eccentricity tides, the inclinations of Saturn’s mid-sized moons are not expected to evolve appreciably over the age of the Solar System. The final inclination of Dione is always substantial, typically comparable to a degree, while the observed inclination of Dione is only  $0.028^\circ$ . So the authors conclude that Tethys and Dione have never crossed this mutual resonance, and that one way to solve this paradox would be that they are younger. Thus they propose that a “proto-Rhea” would have crossed a resonance with “proto-Dione” about 100 Myr ago. The proto-Rhea may have been already placed on an eccentric orbit due to an evection resonance with the Sun. Proto-Rhea and proto-Dione could have collided with a velocity of about 3 km/s, enough to catastrophically disrupt both satellites, and releasing enough material to create a new generation of satellites, plus the rings. This scenario, however, has not been fully tested numerically. Several problems may prevent the debris disk from forming today’s rings. Whereas the spreading timescale of the debris down to the Roche limit may be as fast as 1000 years, the concurrent reaccretion into satellites may act on a similar timescale, leading to a stopping of the spreading process and feeding of the Roche Limit. Also, how the debris could spread all the way to inside  $r_R$ , across the orbits of Enceladus and Mimas, is unclear, as is how the process would produce rings that are overwhelmingly icy. So, while it is clear that a large part of the debris disk would reaccrete into satellites, it is not clear if a small fraction would form Saturn’s rings before being accreted by the satellites. This interesting scenario must be studied in more detail in the future. Beyond the specific case of Dione and Rhea, the Ćuk et al. (2016) paper emphasizes the possible role of evection resonances in Saturn’s satellite system that may regularly destabilize the system, and possibly lead to the destruction and re-accretion of several generations of satellites over the age of the Solar System.

### 18.3.3.10 What would we need to make further progress on the origin of Saturn’s rings?

We have mentioned different possible scenarios for the origin of Saturn’s rings. The main problem to compare them on an equal ground is that they do not have all the same

level of maturity. Some scenarios for ring and satellite origin have been studied in different papers, mixing numerical simulations and semi-analytical models, while others are still based only on qualitative arguments (like the young rings model). In addition, the structure of a circumplanetary disk is still not well constrained. So the first thing we would need to make further progress is a modeling effort on the least explored aspects, including the structure of the circumplanetary disk, as well as a better understanding of the giant planet formation process in the context of the early Solar System. Then we would need new data. Today it is still difficult to design a critical observable that would help to distinguish between these models. Clearly a precise determination of the micro-meteoroid flux at Saturn would help to give surface ages for the rings and satellites. We await the publication of the dust flux onto the rings by Cassini's CDA team. The "grail" would be a sample return from Saturn's rings, but that may not happen for many years.

## 18.4 Rings of Jupiter, Uranus and Neptune

### 18.4.1 Rings of Jupiter

The jovian rings are the only known example of a system comprised solely of "ethereal" rings (Burns et al., 1984). That is, while Jupiter has distinct main and halo rings and two "gossamer" rings, all of these components have optical depths  $\tau \ll 1$ , so that the rings do not present enough surface area to be detected by occultation experiments, but only in images, most easily when the rings are viewed nearly edge-on. Saturn, Uranus, and Neptune all have ethereal rings too, but in addition have rings of higher  $\tau$ . Ethereal rings consist largely, or in some cases almost entirely, of "dust," particles with sizes in the range of 0.1–100  $\mu m$ . Dust particles are subject to non-gravitational forces (Burns et al., 1984, 2001) such as Poynting-Robertson drag, radiation pressure and electromagnetic forces.

Jupiter has four known moons within the orbit of the innermost galilean satellite, Io – moving outward, Metis, Adrastea, Amalthea, and Thebe. The two gossamer rings, with optical depths of order  $10^{-7}$  and  $10^{-8}$ , are clearly associated with Amalthea and Thebe because the rings' outer edges coincide with the orbits of the two moons. In addition, the thicknesses of the gossamer rings match the vertical excursions of Amalthea and Thebe from Jupiter's equatorial plane (thousands of km) due to their slightly inclined orbits. The gossamer rings have been interpreted as dust liberated from Amalthea and Thebe by micrometeoroid impacts that evolves inward under Poynting-Robertson (P-R) drag (Burns et al., 1999; Showalter et al., 2007). For micron-sized particles, the P-R drag timescale is  $\approx 10^5$  years (Burns et al., 1984, 2004).

Moving inward from the gossamer rings, the "main" jovian ring is roughly bounded by Metis and Adrastea, which are much smaller than Amalthea and Thebe. The optical depths in macroscopic particles  $\tau_L$  and in dust  $\tau_S$  in the main ring are comparable. For instance, Throop et al. (2004)

find  $\tau_L \approx 4.7 \times 10^{-6}$  and  $\tau_S \approx 1.3 \times 10^{-6}$ . Metis and Adrastea are important sources for the main ring, but unlike the gossamer ring, additional source bodies must be present. Burns et al. (2004) estimate that the two moons "comprise only about one-third of the [main] ring's total area in source bodies." Metis and Adrastea have much smaller orbital inclinations than Amalthea and Thebe, and the main ring is physically much thinner (of order 100 km), compared with the gossamer rings.

Finally, the innermost jovian ring is the "halo," which has a wide radial extent ( $\approx 30,000$  km), with its outer edge near the inner edge of the main ring. The halo is physically thick; although most of the particles in the halo lie within a few hundred km of Jupiter's equatorial plane, the halo is still detectible 10,000 km from the plane. The radial extent of the halo is bounded approximately by the 2:1 Lorentz resonance and the 3:2 Lorentz resonance at 1.41 and 1.71 Jupiter radii, respectively. Lorentz resonances involve a relationship between a particle's orbital frequency and the rate at which Jupiter (and its magnetic field) rotate. For instance, at the 3:2 Lorentz resonance, a particle completes three orbits for every two rotations of Jupiter. Lorentz resonances can have large effects on small, charged particles. Ring particles can be charged by interacting with electrons and ions trapped in Jupiter's magnetosphere, with electrons in Jupiter's extended ionosphere, and via the photoelectric effect due to sunlight.

The lifetimes of individual particles in the jovian rings are much shorter than the age of the Solar System, so the particles must be resupplied by impacts into, and perhaps between, larger parent bodies. Sputtering, i.e., erosion through impacts of fast ions or atoms onto solid bodies, is thought to be the most important loss mechanism for dust particles in the rings. A "fast drag" model (Horányi and Cravens, 1996; Horányi and Juhász, 2010) predicts much more rapid loss of individual ring particles, and a somewhat different spatial distribution of ring material than the work described above. Observations by the Juno spacecraft, which went into orbit around Jupiter in July 2016, may be able to distinguish between the competing models.

### 18.4.2 Rings of Uranus and Neptune

The rings of Uranus and Neptune, although much less explored than those of Saturn, have origins that seem easier to understand than Saturn's rings. The uranian and neptunian rings are much less massive than Saturn's and show a complex structure in which numerous small satellites orbit near the rings. Each ring system contains one or more narrow, relatively dense ringlets and wide tenuous dust belts. Ringlet optical depths range from  $10^{-6}$  to  $\mathcal{O}(1)$  for Uranus and from  $10^{-4}$  to 0.1 for Neptune. Uranus has 13 small satellites in the vicinity of its ring system; all except Cordelia orbit outside of the most opaque ringlet, the  $\epsilon$  ring. Cordelia and Ophelia are thought to shepherd the  $\epsilon$  ring (Porco and Goldreich, 1987; Goldreich and Porco, 1987; Chiang and Goldreich, 2000; Mosqueira and Estrada, 2002). Neptune has 6 small satellites near its ring system; four of the six orbit interior to its densest ring, the Adams ring. The three arcs within

the Adams ring appear to have a resonant relationship with the moon Galatea (Porco, 1991; Sicardy et al., 1999; Dumas et al., 1999; Namouni and Porco, 2002), but the arcs changed in a decade for reasons that are not well understood (de Pater et al., 2005).

The close dynamical association of Uranus and Neptune’s rings with the population of small moons fueled the idea that these rings may derive from the satellites themselves. In addition, the mass of the uranian rings is estimated to be comparable to a 10–20 km moonlet for a density  $\simeq 1 \text{ g/cm}^3$ , and the neptunian rings are probably much less massive yet (Esposito et al., 1991). The “ring moons” of Uranus and Neptune have radii of about 10–100 km. Thus, in principle, there is enough material in the satellites for them to be a source for ring material through a process of surface erosion or destruction via meteoroid bombardment. Incomplete re-accretion due to tides (Canup and Esposito, 1995) may provide a natural explanation for the coexistence of rings and moons (see also Crida, 2015; Hyodo and Ohtsuki, 2015).

In a series of papers, Colwell and Esposito have explored the effect of meteoroid bombardment on the inner moons of Uranus and Neptune (Colwell and Esposito, 1990a,b, 1992, 1993). They show that meteoroid impacts on moons orbiting a giant planet may have a completely different outcome than, for example, asteroid collisions. First, the impact velocity of a passing body coming from orbit around the Sun is very high, typically 20 km/s, due to the gravitational focusing induced by the giant planet. By comparison, the average impact velocity in the asteroid belt is about 5 km/s. So every impact on a moon is much more violent, as the impact energy scales with the square of the impact velocity. Second, as the small moons orbit close to their planets, the sizes of their Hill spheres (i.e., their spheres of gravitational influence) are comparable to their physical sizes (see section 18.2.4). Inside the Roche limit, the Hill sphere is comparable to or smaller than the physical size of the body. Just above the Roche limit, the Hill sphere of a satellite is only a little bigger than the size of the satellite. This implies that most of the material launched by meteoroid impact is easily lost because of the tidal field of the host planet, especially below the Roche limit. As a result, debris produced after the erosion or destruction of a moonlet will reaccumulate with difficulty, or after a long timescale (many orbital periods). Between destruction of a moon and re-accretion, debris in orbit around the host planet will slowly spread longitudinally and will progressively form a ring.

After an impact, the ejecta from a moon with semi-major axis  $a$  will scatter around their ejection point with a radial width  $\Delta a/a \approx V_e/V_{\text{orb}}$ , where  $V_e$  is the ejection velocity,  $V_{\text{orb}}$  is the moon’s orbital velocity, and  $\Delta a$  is the radial spread of the ejecta. Colwell and Esposito (1993) compute that impact ejecta larger than  $\approx 1 \text{ cm}$  should gather in ringlets about 50 km wide, comparable to the observed widths of the narrow rings of Uranus and Neptune. However, over timescales of many orbital periods, collisions between fragments will spread the ring. In addition, effects including Poynting–Robertson drag (Burns et al., 2001) and exospheric drag (Colwell and Esposito, 1993; Esposito et al., 1991) may cause the orbits of ring material to evolve.

Colwell and Esposito (1992), Colwell et al. (2000), and Zahnle et al. (2003) have estimated the rate of catastrophic disruption of the moons of the giant planets, assuming the impactors are comets (“Centaur”). The model rates are derived by combining crater size-frequency distributions measured on moons of the giant planets by Voyager with theoretical extrapolations of the number of comets observed in the inner Solar System. Under two different assumptions for the impactors’ size distribution, Zahnle et al. (2003) find that all of Uranus’s inner moons within Puck’s orbit should have been destroyed, on average, in the past  $\approx 0.3$  to 2.5 Gyr. The same calculation for Neptune’s satellites shows that all inner moons inside Proteus’s orbit may have been destroyed in the past  $\approx 0.3$  to 3.5 Gyr (Zahnle et al., 2003). These destruction timescales are estimated by assuming *current* impact rates, with a modest increase as one goes further into the past. The impactor flux may have been much larger long ago, due either to post-accretional bombardment just after the formation of the giant planets, or much later, due to major dynamical instabilities in the Solar System, perhaps some  $\sim 650 \text{ Myr}$  after the Solar System formed during the “Late Heavy Bombardment” (Gomes et al., 2005; Charnoz et al., 2009a).

So Uranus and Neptune’s current ring-satellite systems may be in a cycle of accretion and destruction. Even if the structures we see today are young (with ages comparable to destruction timescales), the material they are made of may be as old as the planets themselves. In addition, because the synchronous orbits of Uranus and Neptune are, except for Uranus’s tenuous  $\mu$  ring, beyond their ring systems (about 3.3 and 3.4 planetary radii for Uranus and Neptune, respectively), the planet-induced tidal evolution of their satellites close to the rings is inward. Thus Uranus and Neptune’s inner satellites cannot escape the ring region (which is opposite to the case of Saturn, for which all satellites finally escape the ring region, see section 18.3.3.7), so this ring-satellite cycle can continue for as long as there is material in the ring region. For the uranian rings, the drag from the planet’s extended atmosphere (Esposito et al., 1991) may be the most important mechanism for removing material from the rings.

However, the current ring systems may, in terms of their total mass, be insignificant compared to early ring systems that might have existed around the ice giants. An intriguing recent proposal (Crida and Charnoz, 2012) suggests that Uranus and Neptune originally had massive rings comparable to Saturn’s, and that these rings gave birth to the regular satellites of the ice giants. This claim is supported by the similar mass-distance relationship in these three satellite systems (where the mass grows roughly as the distance to the Roche limit squared), which fits well with the theoretical distribution expected from the spreading of rings beyond the Roche limit. If true, the rings of Saturn, Uranus and Neptune could have a similar origin; the question then becomes: why are they well below the asymptotic mass described in section 18.2.2 around the ice giants and not around Saturn?

The uranian ring-satellite system poses a specific challenge because of the high obliquity of Uranus ( $\approx 98^\circ$ ; i.e., Uranus is roughly “on its side,” with its rotation poles near



its orbital plane). In our current understanding of planet formation, it is unlikely that Uranus formed with such a large obliquity. Uranus’s high obliquity may be due to an event occurring after the planet formed. Because Uranus’s system of rings and satellites lies in its equatorial plane, either (i) they must have formed after Uranus acquired its obliquity or (ii) the process that tilted Uranus must have also been able to tilt its ring and satellite system if they were already present. Models for tilting Uranus include a collisionless scenario involving a massive inclined satellite (Boué and Laskar, 2010), or oblique collisions with nearby protoplanets (e.g. Morbidelli et al., 2012).

In the collisionless scenario, Uranus’s spin is slowly tilted by a resonance between the precession rates of its spin axis and of its orbital plane, and the satellites adiabatically follow the equatorial plane of the planet. However, such a resonance requires the presence a massive satellite ( $10^{-3}$ – $10^{-2}$  times the mass of Uranus) at about 0.01 AU (about  $60R_U$ , where  $R_U$  is the radius of Uranus), compared with  $23R_U$  for Oberon, the outermost regular moon) to speed up the known moons’ precession rates (Boué and Laskar, 2010). But this distant satellite would stay in the ecliptic plane, and would keep the outermost of the other satellites (Oberon and Titania) in orbits near this plane as well. This massive satellite, not being observed today, must be ejected at some point. When this happens, Oberon and Titania would retain high inclinations relative to Uranus’ equatorial plane, inconsistent with their current extremely low inclinations.

In the collisional scenario, the impact tilts the planet suddenly, but not the satellite system. The impact also produces a compact, massive disk of ejecta in the new equatorial plane of the planet (Slattery (1992); called the C-ring by Morbidelli et al. (2012)). This dramatically increases Uranus’s effective  $J_2$ , and forces a pre-existing proto-satellite disk or satellite system to precess incoherently about the new equatorial plane. The randomization of the nodes leads to collisions and damping, so that a debris disk forms in the new equatorial plane. Note that if the planet’s tilt is more than  $90^\circ$ , the new debris disk would be retrograde, so that Uranus must begin with a modest non-zero obliquity, and thus at least two obliquity-producing collisions are then needed for Uranus’s prograde system. The present satellites and rings of Uranus then form from this new debris disk, while the satellites formed by the spreading of the C-ring beyond the Roche limit would be pulled back inwards by Uranian tides (as they would lie inside the synchronous orbit) (Morbidelli et al., 2012). However, one could envision that resonant interactions between these satellites born from the C-ring could push them beyond the synchronous orbit (see, for instance, Salmon and Canup, 2015), in which case no pre-existing proto-satellite disk or satellite system would be needed, following Crida and Charnoz (2012), so long as the tidal  $Q_p$  parameter for Uranus was low enough to drive satellites outward to Oberon’s distance. Then, perhaps Uranus’s present rings could be small remnants of the C-ring, and only one giant impact might be enough<sup>4</sup>. In any case, the disappearance

of the C-ring should be studied to understand the origin of present rings of Uranus. It is also possible that Uranus once had massive rings that were entirely lost, with the current rings produced subsequently.

Whereas we seem to understand the close relation between the rings and satellites, and have identified a cycle of material between the two, we must ask which came first, the rings or the satellites? This “chicken and egg” problem points to *the* key question for every ring formation model: how to put material within a planet’s Roche limit? A handful of scenarios have been considered, at least for Saturn (see section 18.3.3). For Uranus and Neptune, only a couple of studies have considered this question. First, a collision with a nearby protoplanet could do the job (Slattery, 1992; Morbidelli et al., 2012). Another alternative is through a cometary bombardment during the LHB, but it appears that the mass injected into the Uranus and Neptune systems may be much higher than is currently observed (Charnoz et al., 2009b). Thus, for the moment, there is still great uncertainty on the origin and evolution of the ring systems of Uranus or Neptune, notably including the potential for earlier more massive rings.

## 18.5 Other Ring Systems

### 18.5.1 Centaurs

The asteroid (10199) Chariklo is the largest known Centaur. Its figure can be fit with a slightly oblate spheroid of equivalent radius 127 km (Braga-Ribas et al., 2014). Chariklo orbits between Saturn and Uranus, with a semi-major axis of 15.8 AU and an eccentricity of 0.17. Braga-Ribas et al. (2014) observed a stellar occultation by this object from ten observatories in South America. Before and after the occultation by the main body of Chariklo, one or two brief extinctions of the background star were observed. At La Silla, the light curve had enough time resolution (10 Hz) to clearly see two brief consecutive occultations on either side of the main body. These results imply that Chariklo has two rings, with widths of  $\approx 7$  and 3 km and optical depths of  $\approx 0.4$  and 0.06, separated by 14 km in distance from Chariklo. The rings are about 400 km from the center of Chariklo. The rings lie near Chariklo’s Roche limit if Chariklo has a density near  $1 \text{ g/cm}^3$  (the mass of Chariklo is not well constrained). We refer the reader to Chapter 7 for a detailed description of rings around Centaurs.

The existence of such rings is surprising. Although Braga-Ribas et al. (2014) show that Chariklo is unlikely to have undergone an encounter so close to a giant planet that it would have disrupted pre-existing rings, the question of their formation and evolution remains open. The rings’ apparent confinement suggests that they may be shepherded by moonlets, as Saturn’s narrow F ring is flanked by Prometheus and Pandora. Unfortunately, our incomplete knowledge of the Chariklo system, which might have moons or other rings, provides no clue as to a possible progenitor for the rings, nor for their age. The rings appear to have sharp edges; uncon-

<sup>4</sup> Note that the same scenario could apply to Neptune’s system and its  $30^\circ$  inclination.

finned rings would spread rapidly, but shepherded satellites could maintain sharp edges for a long time. Narrow rings are also found around Saturn, Uranus, and Neptune, but it seems difficult to find a formation mechanism that would apply to giant planets as well as to Centaurs.

Pan and Wu (2016) consider three mechanisms for the origin of Chariklo’s rings – a cratering event that lofted material into orbit within the Roche limit when Chariklo was still in the Kuiper Belt; an encounter with a giant planet that perturbed a small moon inward of the Roche limit; and lofting of dust particles from Chariklo due to cometary activity. The third mechanism is novel. In this scenario, CO or N<sub>2</sub> outgasses from Chariklo’s interior as the body warms during its journey from the Kuiper Belt to its current orbit between 13 and 19 AU. Seasonal outgassing might lift fine dust from Chariklo’s surface, with a small fraction ending up in stable orbits around the Centaur. Subsequent collisional evolution of dust and condensates is required to form the few-meter-sized particles that Pan and Wu (2016) estimate to be present in the rings. An interesting aspect of the outgassing model is that it predicts that rings may be common around Centaurs, whereas they should be uncommon or absent for KBOs, which are not known to display cometary activity. Such an observational prediction may be checked with future systematic transit observations of KBOs and Centaurs. However, how outgassing or cratering would produce narrow circular rings is not clear at all.

Ortiz et al. (2015) and Ruprecht et al. (2015) reported possible ring material around another large Centaur, Chiron. Like Chariklo’s rings, the features observed near Chiron were detected by means of stellar occultations. However, the case that Chiron has rings is not as certain, because, unlike Chariklo, Chiron displays cometary activity, so that dips seen away from the Centaur might instead be due to material ejected from the nucleus, and not orbiting it. A ring system around yet another large Centaur, Bienor, has recently been suggested, based on photometry (Fernández-Valenzuela et al., 2016).

An alternative process was recently proposed to explain the presence of rings around Centaurs. Using SPH simulations, Hyodo et al. (2016) showed that a Centaur experiencing a close encounter with a giant planet (within 1.8 planetary radii) may be substantially tidally disrupted, but without being fully destroyed. A fraction of the resulting cloud of debris remains gravitationally bound to the Centaur as the latter flies away from the giant planet. The debris then flattens into a ring. This process has the advantage of being generic. As Centaurs are believed to be objects from the Kuiper Belt scattered by giant planets inside Neptune’s orbit, such events may have happened in the past. However, very close encounters are needed and the rate of such very close encounters is not yet clear, so the probability of such a scenario still needs to be evaluated in the future. In addition, the evolution of a debris disk into a couple of very narrow rings is still unclear. Perhaps satellite formation occurring inside the debris disk may lead to radial confinement of material.

### 18.5.2 Exo-rings

Since the discovery of the exoplanet 51 Pegasi b in 1995, there have been tremendous efforts to discover new planets, either from the ground (e.g. HARPS, WASP) or from space (e.g. CoRoT, Kepler, CHEOPS). Thus far, about 2000 exoplanets have been confirmed, and thousands of others await confirmation in various observing programs. Of course, there is, a priori, no reason to believe that rings are specific to giant planets in our Solar System. We would naturally expect that rings may be found around exoplanets. However, the known exoplanets are, in general, quite different from the giant planets in our Solar System, primarily because detection techniques still do not allow efficient detection of Solar System-like planets. These biases may imply that rings are rare around the *known* exoplanets. Specifically, most planets found via the most common techniques, radial velocity measurements or transits, are very close to their central stars, well within 0.5 AU. In addition, statistically, Earth-sized and Neptune-sized planets are more abundant than giant planets (see, e.g., Lissauer et al., 2014; Martin and Livio, 2015). These configurations impose unusual dynamical and physical conditions on the existence of rings around confirmed exoplanets.

First of all close to the star we are well inside the snow line, so that only rings made of refractory material (like silicate minerals) can survive. Such rings may be very different from Saturn’s icy rings. “Refractory” rings will be comprised of denser particles, and should orbit closer to their host planets, compared to our Solar System, due to the reduced size of the Roche limit (see Eq. 18.2) for silicate material.

Second, rings lie in the Laplace plane, that is, the mean orbital plane above and below which inclined orbital planes precess. This opens the possibility for warped rings, as the Laplace plane coincides with the planet’s equatorial plane close to the planet, but shifts to the planet’s orbital plane further out. Burns (1986) and Tremaine et al. (2009) show that the distance below which rings should lie in the planet’s equatorial plane is:

$$R_l = R_p (J_2/q)^{1/5}, \quad (18.10)$$

with  $R_p$  standing for the planet’s radius, and  $q = (M_*/M_p)(M_*/a_p)^3$ , with  $M_*$ ,  $M_p$ , and  $a_p$  standing for the star’s mass, planet’s mass, and distance to the star, respectively. Close to the star, a planet may be synchronously rotating, in which case there is a simple relation between its  $J_2$  and  $q$ :  $J_2 = \frac{5}{6}k_2q$  (Correia and Rodríguez, 2013). Then,  $R_l$  simplifies to  $R_l = R_p(\frac{5}{6}k_2)^{1/5}$ . Noting that  $k_2$  (the Love number) is, in general, close to 0.5 (see, e.g. Yoder, 1995), we find  $R_l \approx 0.84R_p$ . The conclusion is that planets orbiting synchronously with their host star would not have their rings in their equatorial planes, but rather in their orbital planes<sup>5</sup>. This may make ring detection by transit difficult, as such rings would be seen edge-on.

Claimed detections of exo-rings are few and are all a matter of debate because of their intrinsic difficulty. Kenworthy

<sup>5</sup> These two planes may, however, be the same, as synchronous rotation is often accompanied by alignment of the spin axis with the orbital axis.

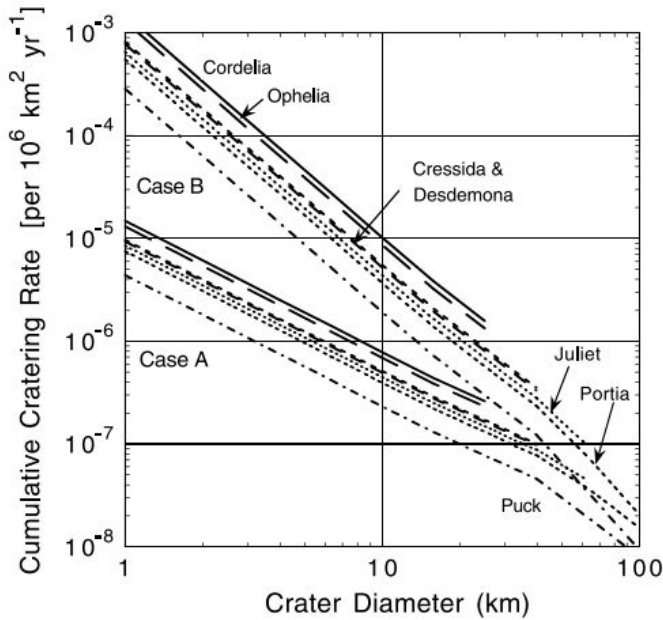


**Figure 18.6** Actual bombardment rates of Uranus' inner moons. Adapted from Zahnle et al. (2003).

and Mamajek (2015) report the detection via transit of an exo-ring system around an unseen companion of a pre-main sequence K5 star. However, the detected ring system seems to fill the companion's Hill sphere. Whereas the structure may indeed exist, its extent and the star's age instead suggest either a circumstellar or a circumplanetary disk rather than a typical ring system dominated by tides. The existence of a ring system around Fomalhaut b (a planet orbiting at about 115 AU from its host star) has been suggested to explain the unexpected brightness of the object (Kalas et al., 2008). However, to fully account for the observed brightness, a ring system as wide as 35 planet radii seems necessary. So, again, this may be rather a circumplanetary structure than a ring system.

## 18.6 Conclusion

Do we know how planetary rings are formed? Well, we have to admit that this is still an open question. The last three decades of exploration of our Solar System's planets have shown how diverse and how complex the different planetary ring systems are. In the past decade, the close association of ring evolution with satellite formation was identified and allowed us to make significant progress in our understanding of rings. Whereas we are still not sure of the process of ring formation, we envision several possible different scenarios, but each faces its own problems. The most difficult questions to address include:

- Why are the rings around the four giant planets so different?
- Why do they all revolve in the prograde direction?

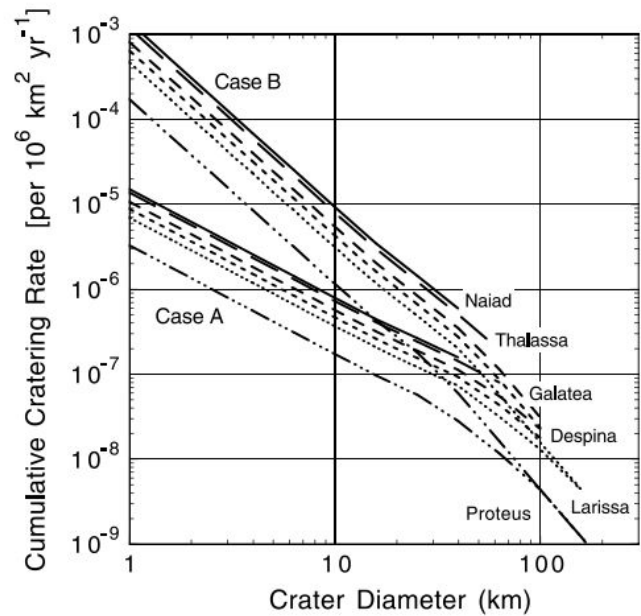


**Figure 18.7** Actual bombardment rates of Neptune's inner moons. Adapted from Zahnle et al. (2003).

- Why are Saturn's rings so ice-rich, while those of Uranus and Neptune seem to be made of a non-icy material?
- Why are Saturn's rings orders of magnitude more massive than the other ring systems, despite potentially common formation processes?
- Why don't terrestrial planets have rings?

The challenge is creating a ring formation scenario that allows enough variability to explain the wide diversity of planetary rings. Perhaps there is no unique scenario to form rings, so that every planet may have a different history. For the case of Saturn, it seems that tidal stripping from the outer ice shell of an ancient differentiated satellite, collisional disruption of a pre-existing small moon, or tidal disruption of the outer icy layers of a differentiated planetary interloper may all represent viable formation mechanisms in case the rings are as old as Saturn itself. But when and how such events occurred is still uncertain. For tidal stripping from an inwardly migrating satellite to produce a long-lived ring, there must be a favorable agreement in timing between satellite migration and the disappearance of the circumplanetary disk in order for the ring to survive against gas drag. Perhaps Saturn's ring was the only one to achieve such conditions, with thus-formed massive rings at the other planets destroyed. If Saturn's rings formed by the total disruption of a small moon, early tidal evolution at Saturn must have been slow, and an explanation is needed as to why the rings (and many of the medium-sized inner satellites) are so ice-rich, rather than a mixture of rock and ice as expected for solar abundances. We still await the results of the CDA instrument on Cassini, which will help to constrain the pollution timescale of Saturn's rings. If Saturn's rings formed by the tidal disruption of the outer layers of differentiated comets or large KBOs that made close passages during the LHB, then we see no reason why the outer planet ring systems

would all orbit in the prograde direction, nor why the other giant planets would lack massive ring systems today.

Whereas the exact timing of these scenarios is unknown, they all imply that either the rings formed concurrently with Saturn or that they formed during a phase of intense bombardment of the outer Solar System, the so-called Late Heavy Bombardment that may have happened about 3.8 Gyr ago. Forming rings in a much more recent period seems a difficult task, as we do not know any major restructuring event of the Solar System in, at least, the last 3 Gyr. However, Čuk et al. (2016) emphasize that evection resonances of some of Saturn’s moons with the Sun may have lead recently to resonantly-driven collisions in the system. During such destructive collisions among satellites, massive disks of debris may form and may re-accrete into a new generation of moons and, putatively, could create a young ring system. This scenario has not been tested numerically and we view it as unlikely that it will be able to reproduce the observed mass-distance distribution of Saturn’s moons as well as the ice-rich composition of the rings.

Perhaps for Uranus and Neptune giant impacts played an additional role in modifying the final systems. We think that the Earth suffered a giant impact that gave birth to our Moon via a Roche interior disk (Cameron and Ward, 1976; Kokubo et al., 2000; Canup and Asphaug, 2001; Crida and Charnoz, 2012; Charnoz and Michaut, 2015), and perhaps Mars’ small moons formed in a similar way (Rosenblatt and Charnoz, 2012; Rosenblatt et al., 2016). Terrestrial rings may have been lost due to the stronger effects of the Sun’s radiation at their smaller semi-major axes, but this has yet to be explored. The perturbations from the Earth’s very massive Moon (Cameron and Ward, 1976; Kokubo et al., 2000), and the inwards tidal migration of Mars’s satellites (Rosenblatt et al., 2016) could also explain how these two planets lost completely their rings.

Developments since 2010 have shown that the rings’ evolution, since it is linked to the satellites’ evolution, is also coupled to the planet’s internal structure, as it is the latter that controls the intensity of tidal dissipation. So it seems that the rings, satellites, and planet form a single system with a strong degree of coupling between its different components. Juno, now in orbit at Jupiter to study the planet’s interior, or JUICE, which is scheduled to go into orbit around Jupiter in 2030, will undoubtedly provide invaluable information on the Jupiter system, which we hope will, in turn, place new constraints on the origin of planetary rings.

Finally, whereas exo-rings have still not been clearly detected, they should be discovered in the next few years. Exo-rings may be detected in transit if the host planet does not orbit too close to its star. The CHEOPS and PLATO missions, with launches planned for 2018 and 2024, may detect such structures. If exo-rings are found around some type of exoplanets, and not others, this may again put constraints on their origin. In the near future, the James Webb Space Telescope, which should be launched in 2018, will have the capability to image rings around exoplanets far from their parent stars. Undoubtedly, our understanding of the origin of planetary rings should advance substantially in the next few years.

## 18.7 Acknowledgements

SC acknowledges the financial support of the UnivEarthS Labex program at Sorbonne Paris Cité (ANR-10-LABX-0023 and ANR-11-IDEX-0005-02). RMC acknowledges support from NASA’s Planetary Geology and Geophysics program. LD thanks the Cassini project and NASA’s Outer Planets Research program for support.

## REFERENCES

- Aggarwal, H. R., and Oberbeck, V. R. 1974. Roche Limit of a Solid Body. *Astrophys. J.*, **191**(July), 577–588.
- Alibert, Y., Mousis, O., and Benz, W. 2005. Modeling the Jovian subnebula. I. Thermodynamic conditions and migration of proto-satellites. *Astron. Astrophys.*, **439**(Sept.), 1205–1213.
- Alvarellos, J. L., Zahnle, K. J., Dobrovolskis, A. R., and Hamill, P. 2005. Fates of satellite ejecta in the Saturn system. *Icarus*, **178**(Nov.), 104–123.
- Asphaug, E., and Benz, W. 1996. Size, Density, and Structure of Comet Shoemaker-Levy 9 Inferred from the Physics of Tidal Breakup. *Icarus*, **121**(June), 225–248.
- Barr, A. C., and Canup, R. M. 2010. Origin of the Ganymede-Callisto dichotomy by impacts during the late heavy bombardment. *Nature Geosci.*, **3**(Mar.), 164–167.
- Benz, W., and Asphaug, E. 1999. Catastrophic Disruptions Revisited. *Icarus*, **142**(Nov.), 5–20.
- Boué, G., and Laskar, J. 2010. A Collisionless Scenario for Uranus Tilting. *Astrophys. J. Lett.*, **712**(Mar.), L44–L47.
- Braga-Ribas, F., Sicardy, B., Ortiz, J. L., Snodgrass, C., Roques, F., Vieira-Martins, R., Camargo, J. I. B., Assafin, M., Duffard, R., Jehin, E., Pollock, J., Leiva, R., Emilio, M., Machado, D. I., Colazo, C., Lellouch, E., Skottfelt, J., Gillon, M., Ligier, N., Maquet, L., Benedetti-Rossi, G., Gomes, A. R., Kervella, P., Monteiro, H., Sfair, R., El Moutamid, M., Tancredi, G., Spagnotto, J., Maury, A., Morales, N., Gil-Hutton, R., Roland, S., Ceretta, A., Gu, S.-H., Wang, X.-B., Harpsøe, K., Rabus, M., Manfroid, J., Opitom, C., Vanzi, L., Mehret, L., Lorenzini, L., Schneiter, E. M., Melia, R., Lecacheux, J., Colas, F., Vachier, F., Widemann, T., Almenares, L., Sandness, R. G., Char, F., Perez, V., Lemos, P., Martinez, N., Jørgensen, U. G., Dominik, M., Roig, F., Reichart, D. E., Lacluyze, A. P., Haislip, J. B., Ivarsen, K. M., Moore, J. P., Frank, N. R., and Lambas, D. G. 2014. A ring system detected around the Centaur (10199) Chariklo. *Nature*, **508**(Apr.), 72–75.
- Burns, J. A. 1986. The evolution of satellite orbits. Pages 117–158 of: Burns, J. A., and Matthews, M. S. (eds), *IAU Colloq. 77: Satellites*.
- Burns, J. A., Showalter, M. R., and Morfill, G. E. 1984. The ethereal rings of Jupiter and Saturn. Pages 200–272 of: Greenberg, R., and Brahic, A. (eds), *IAU Colloq. 75: Planetary Rings*.
- Burns, J. A., Showalter, M. R., Hamilton, D. P., Nicholson, P. D., de Pater, I., Ockert-Bell, M. E., and Thomas, P. C. 1999. The Formation of Jupiter’s Faint Rings. *Science*, **284**(May), 1146.
- Burns, J. A., Hamilton, D. P., and Showalter, M. R. 2001. Dusty Rings and Circumplanetary Dust: Observations and Simple Physics. Pages 641–725 of: Grün, E., Gustafson, B. A. S., Dermott, S., and Fechtig, H. (eds), *Interplanetary Dust, Berlin: Springer*.
- Burns, J. A., Simonelli, D. P., Showalter, M. R., Hamilton, D. P., Porco, C. D., Throop, H., and Esposito, L. W. 2004. Jupiter’s ring-moon system. Pages 241–262 of: Bagenal, F., Dowling, T. E., and McKinnon, W. B. (eds), *Jupiter. The Planet, Satellites and Magnetosphere*.
- Cameron, A. G. W., and Ward, W. R. 1976 (Mar.). The Origin of the Moon. In: *Lunar and Planetary Science Conference. Lunar and Planetary Science Conference*, vol. 7.
- Canup, R. M. 2010. Origin of Saturn’s rings and inner moons by mass removal from a lost Titan-sized satellite. *Nature*, **468**(Dec.), 943–946.
- Canup, R. M. 2013 (Mar.). Modification of the Rock Content of the Inner Saturnian Satellites by an Outer Solar System LHB. Page 2298 of: *Lunar and Planetary Science Conference*, vol. 44.
- Canup, R. M., and Asphaug, E. 2001. Origin of the Moon in a giant impact near the end of the Earth’s formation. *Nature*, **412**(Aug.), 708–712.
- Canup, R. M., and Esposito, L. W. 1995. Accretion in the Roche zone: Coexistence of rings and ring moons. *Icarus*, **113**(Feb.), 331–352.
- Canup, R. M., and Esposito, L. W. 1996. Accretion of the Moon from an Impact-Generated Disk. *Icarus*, **119**(Feb.), 427–446.
- Canup, R. M., and Ward, W. R. 2002. Formation of the Galilean Satellites: Conditions of Accretion. *Astron. J.*, **124**(Dec.), 3404–3423.
- Canup, R. M., and Ward, W. R. 2006. A common mass scaling for satellite systems of gaseous planets. *Nature*, **441**(June), 834–839.
- Charnoz, S., and Michaut, C. 2015. Evolution of the protolunar disk: Dynamics, cooling timescale and implantation of volatiles onto the Earth. *Icarus*, **260**(Nov.), 440–463.
- Charnoz, S., Morbidelli, A., Dones, L., and Salmon, J. 2009a. Did Saturn’s rings form during the Late Heavy Bombardment? *Icarus*, **199**(Feb.), 413–428.
- Charnoz, S., Dones, L., Esposito, L. W., Estrada, P. R., and Hedman, M. M. 2009b. Origin and Evolution of Saturn’s Ring System. Pages 537–575 of: Dougherty, M. K., Esposito, L. W., and Krimigis, S. M. (eds), *Saturn from Cassini-Huygens*.
- Charnoz, S., Salmon, J., and Crida, A. 2010. The recent formation of Saturn’s moonlets from viscous spreading of the main rings. *Nature*, **465**(June), 752–754.
- Charnoz, S., Crida, A., Castillo-Rogez, J. C., Lainey, V., Dones, L., Karatekin, Ö., Tobie, G., Mathis, S., Le Poncin-Lafitte, C., and Salmon, J. 2011. Accretion of Saturn’s mid-sized moons during the viscous spreading of young massive rings: Solving the paradox of silicate-poor rings versus silicate-rich moons. *Icarus*, **216**(Dec.), 535–550.

- Chiang, E. I., and Goldreich, P. 2000. Apse Alignment of Narrow Eccentric Planetary Rings. *Astrophys. J.*, **540**(Sept.), 1084–1090.
- Colwell, J. E., and Esposito, L. W. 1990a. A model of dust production in the Neptune ring system. *Geophys. Res. Lett.*, **17**(Sept.), 1741–1744.
- Colwell, J. E., and Esposito, L. W. 1990b. A numerical model of the Uranian dust rings. *Icarus*, **86**(Aug.), 530–560.
- Colwell, J. E., and Esposito, L. W. 1992. Origins of the rings of Uranus and Neptune. I - Statistics of satellite disruptions. *J. Geophys. Res.*, **97**(June), 10227.
- Colwell, J. E., and Esposito, L. W. 1993. Origins of the rings of Uranus and Neptune. II - Initial conditions and ring moon populations. *J. Geophys. Res.*, **98**(Apr.), 7387–7401.
- Colwell, J. E., Esposito, L. W., and Bundy, D. 2000. Fragmentation rates of small satellites in the outer solar system. *J. Geophys. Res.*, **105**(July), 17589–17600.
- Colwell, J. E., Nicholson, P. D., Tiscareno, M. S., Murray, C. D., French, R. G., and Marouf, E. A. 2009. The Structure of Saturn's Rings. Pages 375–412 of: Dougherty, M. K., Esposito, L. W., and Krimigis, S. M. (eds), *Saturn from Cassini-Huygens*.
- Cook, A. F., and Franklin, F. A. 1970. The Effect of Meteoroidal Bombardment on Saturn's Rings. *Astron. J.*, **75**(Mar.), 195.
- Correia, A. C. M., and Rodríguez, A. 2013. On the Equilibrium Figure of Close-in Planets and Satellites. *Astrophys. J.*, **767**(Apr.), 128.
- Crida, A. 2015. Shepherds of Saturn's ring. *Nature Geosci.*, **8**(Sept.), 666–667.
- Crida, A., and Charnoz, S. 2012. Formation of Regular Satellites from Ancient Massive Rings in the Solar System. *Science*, **338**(Nov.), 1196.
- Crida, A., and Charnoz, S. 2014 (July). Complex satellite systems: a general model of formation from rings. Pages 182–189 of: *IAU Symposium*. IAU Symposium, vol. 310.
- Čuk, M., Dones, L., and Nesvorný, D. 2016. Dynamical Evidence for a Late Formation of Saturn's Moons. *Astrophys. J.*, **820**(Apr.), 97.
- Cuzzi, J. N., and Durisen, R. H. 1990. Bombardment of planetary rings by meteoroids - General formulation and effects of Oort Cloud projectiles. *Icarus*, **84**(Apr.), 467–501.
- Cuzzi, J. N., and Estrada, P. R. 1998. Compositional Evolution of Saturn's Rings Due to Meteoroid Bombardment. *Icarus*, **132**(Mar.), 1–35.
- Cuzzi, J. N., Burns, J. A., Charnoz, S., Clark, R. N., Colwell, J. E., Dones, L., Esposito, L. W., Filacchione, G., French, R. G., Hedman, M. M., Kempf, S., Marouf, E. A., Murray, C. D., Nicholson, P. D., Porco, C. C., Schmidt, J., Showalter, M. R., Spilker, L. J., Spitale, J. N., Srama, R., Sremčević, M., Tiscareno, M. S., and Weiss, J. 2010. An Evolving View of Saturn's Dynamic Rings. *Science*, **327**(Mar.), 1470.
- Daisaka, H., Tanaka, H., and Ida, S. 2001. Viscosity in a Dense Planetary Ring with Self-Gravitating Particles. *Icarus*, **154**(Dec.), 296–312.
- Davidsson, B. J. R. 1999. Tidal Splitting and Rotational Breakup of Solid Spheres. *Icarus*, **142**(Dec.), 525–535.
- de Pater, I., Gibbard, S. G., Chiang, E., Hammel, H. B., Macintosh, B., Marchis, F., Martin, S. C., Roe, H. G., and Showalter, M. 2005. The dynamic neptunian ring arcs: evidence for a gradual disappearance of Liberté and resonant jump of courage. *Icarus*, **174**(Mar.), 263–272.
- Di Sisto, R. P., and Zanardi, M. 2016. Surface ages of mid-size saturnian satellites. *Icarus*, **264**(Jan.), 90–101.
- Dones, L. 1991. A recent cometary origin for Saturn's rings? *Icarus*, **92**(Aug.), 194–203.
- Dones, L., Chapman, C. R., McKinnon, W. B., Melosh, H. J., Kirchoff, M. R., Neukum, G., and Zahnle, K. J. 2009. Icy Satellites of Saturn: Impact Cratering and Age Determination. Pages 613–635 of: Dougherty, M. K., Esposito, L. W., and Krimigis, S. M. (eds), *Saturn from Cassini-Huygens*.
- Dones, L., Brasser, R., Kaib, N., and Rickman, H. 2015. Origin and Evolution of the Cometary Reservoirs. *Space Sci. Rev.*, **197**(Dec.), 191–269.
- Doyle, L. R., Dones, L., and Cuzzi, J. N. 1989. Radiative transfer modeling of Saturn's outer B ring. *Icarus*, **80**(July), 104–135.
- Dumas, C., Terrile, R. J., Smith, B. A., Schneider, G., and Becklin, E. E. 1999. Stability of Neptune's ring arcs in question. *Nature*, **400**(Aug.), 733–735.
- Durisen, R. H. 1984. Transport effects due to particle erosion mechanisms. Pages 416–446 of: Greenberg, R., and Brahic, A. (eds), *IAU Colloq. 75: Planetary Rings*.
- Durisen, R. H. 1995. An instability in planetary rings due to ballistic transport. *Icarus*, **115**(May), 66–85.
- Durisen, R. H., Cramer, N. L., Murphy, B. W., Cuzzi, J. N., Mullikin, T. L., and Cederbloom, S. E. 1989. Ballistic transport in planetary ring systems due to particle erosion mechanisms. I - Theory, numerical methods, and illustrative examples. *Icarus*, **80**(July), 136–166.
- Durisen, R. H., Bode, P. W., Cuzzi, J. N., Cederbloom, S. E., and Murphy, B. W. 1992. Ballistic transport in planetary ring systems due to particle erosion mechanisms. II - Theoretical models for Saturn's A- and B-ring inner edges. *Icarus*, **100**(Dec.), 364–393.
- Durisen, R. H., Bode, P. W., Dyck, S. G., Cuzzi, J. N., Dull, J. D., and White, II, J. C. 1996. Ballistic Transport in Planetary Ring Systems Due to Particle Erosion Mechanisms. III. Torques and Mass Loading by Meteoroid Impacts. *Icarus*, **124**(Nov.), 220–236.
- Elliott, J. P., and Esposito, L. W. 2011. Regolith depth growth on an icy body orbiting Saturn and evolution of bidirectional reflectance due to surface composition changes. *Icarus*, **212**(Mar.), 268–274.
- Esposito, L. W., Brahic, A., Burns, J. A., and Marouf, E. A. 1991. Particle properties and processes in Uranus' rings. Pages 410–465 of: *Uranus*. University of Arizona Press.
- Estrada, P. R., Durisen, R. H., Cuzzi, J. N., and Morgan, D. A. 2015. Combined structural and compositional evolution of planetary rings due to micrometeoroid impacts and ballistic transport. *Icarus*, **252**(May), 415–439.
- Fernandez, J. A., and Ip, W.-H. 1984. Some dynamical aspects of the accretion of Uranus and Neptune - The exchange of orbital angular momentum with planetesimals. *Icarus*, **58**(Apr.), 109–120.
- Fernández-Valenzuela, E., Ortiz, J. L., Duffard, R., Morales, N., and Santos-Sanz, P. 2016. Physical properties of centaur (54598) Bienor from photometry. *Mon. Not. R. Astron. Soc.*, *in press*, Dec.
- Ferrari, C., and Reffet, E. 2013. The dark side of Saturn's B ring: Seasons as clues to its structure. *Icarus*, **223**(Mar.), 28–39.
- Filacchione, G., Ciarniello, M., Capaccioni, F., Clark, R. N., Nicholson, P. D., Hedman, M. M., Cuzzi, J. N., Cruikshank, D. P., Dalle Ore, C. M., Brown, R. H., Cerroni, P., Altobelli, N., and Spilker, L. J. 2014. Cassini-VIMS observations of Saturn's main rings: I. Spectral properties and temperature radial profiles variability with phase angle and elevation. *Icarus*, **241**(Oct.), 45–65.

- Fortney, J. J., Marley, M. S., and Barnes, J. W. 2007. Planetary Radii across Five Orders of Magnitude in Mass and Stellar Insolation: Application to Transits. *Astrophys. J.*, **659**(Apr.), 1661–1672.
- Fuller, J., Luan, J., and Quataert, E. 2016. Resonance locking as the source of rapid tidal migration in the Jupiter and Saturn moon systems. *Mon. Not. R. Astron. Soc.*, **458**(June), 3867–3879.
- Goldreich, P., and Porco, C. C. 1987. Shepherding of the Uranian Rings. II. Dynamics. *Astron. J.*, **93**(Mar.), 730–737.
- Goldreich, P., and Soter, S. 1966. Q in the Solar System. *Icarus*, **5**, 375–389.
- Goldreich, P., and Tremaine, S. 1980. Disk-satellite interactions. *ApJ*, **241**(Oct.), 425–441.
- Goldreich, P., and Tremaine, S. 1982. The dynamics of planetary rings. *Annu. Rev. Astron. Astrophys.*, **20**, 249–283.
- Goldreich, P., and Ward, W. R. 1973. The Formation of Planetesimals. *Astrophys. J.*, **183**(Aug.), 1051–1062.
- Gomes, R., Levison, H. F., Tsiganis, K., and Morbidelli, A. 2005. Origin of the cataclysmic Late Heavy Bombardment period of the terrestrial planets. *Nature*, **435**(May), 466–469.
- Hahn, J. M., and Malhotra, R. 1999. Orbital Evolution of Planets Embedded in a Planetesimal Disk. *Astron. J.*, **117**(June), 3041–3053.
- Harris, A. 1984. The Origin and evolution of planetary rings. Pages 641–659 of: Brahic, A., and Greenberg, R. (eds), *Planetary Rings, Edited by A. Brahic and R. Greenberg, University of Arizona Press, Tucson AZ, pp. 641–659*.
- Hedman, M. M., and Nicholson, P. D. 2016. The B-ring’s surface mass density from hidden density waves: Less than meets the eye? *Icarus*, **279**(Nov.), 109–124.
- Horányi, M., and Cravens, T. E. 1996. The structure and dynamics of Jupiter’s ring. *Nature*, **381**(May), 293–295.
- Horányi, M., and Juhász, A. 2010. Plasma conditions and the structure of the Jovian ring. *J. Geophys. Res. (Space Physics)*, **115**(Sept.), A09202.
- Hyodo, R., and Ohtsuki, K. 2015. Saturn’s F ring and shepherd satellites a natural outcome of satellite system formation. *Nature Geosci.*, **8**(Aug.), 686–689.
- Hyodo, R., Charnoz, S., Genda, H., and Ohtsuki, K. 2016. Formation of Centaurs’ Rings through Their Partial Tidal Disruption during Planetary Encounters. *Astrophys. J. Lett.*, **828**(Sept.), L8.
- Hyodo, R., Charnoz, S., Ohtsuki, K., and Genda, H. 2017. Ring formation around giant planets by tidal disruption of a single passing large Kuiper belt object. *Icarus*, **282**(Jan.), 195–213.
- Ip, W.-H. 1983. Collisional interactions of ring particles - The ballistic transport process. *Icarus*, **54**(May), 253–262.
- Ip, W.-H. 1984. Ring torque of Saturn from interplanetary meteoroid impact. *Icarus*, **60**(Dec.), 547–552.
- Ishiguro, M., Yang, H., Usui, F., Pyo, J., Ueno, M., Ootsubo, T., Minn Kwon, S., and Mukai, T. 2013. High-resolution imaging of the Gegenschein and the Geometric Albedo of Interplanetary Dust. *Astrophys. J.*, **767**(Apr.), 75.
- Jeffreys, H. 1947. The relation of cohesion to Roche’s limit. *Mon. Not. R. Astron. Soc.*, **107**, 260–272.
- Kalas, P., Graham, J. R., Chiang, E., Fitzgerald, M. P., Clampin, M., Kite, E. S., Stapelfeldt, K., Marois, C., and Krist, J. 2008. Optical Images of an Exosolar Planet 25 Light-Years from Earth. *Science*, **322**(Nov.), 1345–1348.
- Kenworthy, M. A., and Mamajek, E. E. 2015. Modeling Giant Extrasolar Ring Systems in Eclipse and the Case of J1407b: Sculpting by Exomoons? *Astrophys. J.*, **800**(Feb.), 126.
- Kirchoff, M. R., and Schenk, P. 2009. Crater modification and geologic activity in Enceladus’ heavily cratered plains: Evidence from the impact crater distribution. *Icarus*, **202**(Aug.), 656–668.
- Kokubo, E., Ida, S., and Makino, J. 2000. Evolution of a Circumterrestrial Disk and Formation of a Single Moon. *Icarus*, **148**(Dec.), 419–436.
- Lainey, V., Arlot, J.-E., Karatekin, Ö., and van Hoolst, T. 2009. Strong tidal dissipation in Io and Jupiter from astrometric observations. *Nature*, **459**(June), 957–959.
- Lainey, V., Karatekin, Ö., Desmars, J., Charnoz, S., Arlot, J.-E., Emelyanov, N., Le Poncin-Lafitte, C., Mathis, S., Remus, F., Tobie, G., and Zahn, J.-P. 2012. Strong Tidal Dissipation in Saturn and Constraints on Enceladus’ Thermal State from Astrometry. *Astrophys. J.*, **752**(June), 14.
- Lainey, V., Jacobson, R. A., Tajeddine, R., Cooper, N. J., Murray, C., Robert, V., Tobie, G., Guillot, T., Mathis, S., Remus, F., Desmars, J., Arlot, J.-E., De Cuyper, J.-P., Dehant, V., Pascu, D., Thuillot, W., Le Poncin-Lafitte, C., and Zahn, J.-P. 2017. New constraints on Saturn’s interior from Cassini astrometric data. *Icarus*, **281**(Jan.), 286–296.
- Latter, H. N., Ogilvie, G. I., and Chupeau, M. 2014. The ballistic transport instability in Saturn’s rings - III. Numerical simulations. *Mon. Not. R. Astron. Soc.*, **441**(July), 2773–2781.
- Levison, H. F., Kretke, K. A., and Duncan, M. J. 2015. Growing the gas-giant planets by the gradual accumulation of pebbles. *Nature*, **524**(Aug.), 322–324.
- Lin, D. N. C., and Papaloizou, J. 1979. Tidal torques on accretion discs in binary systems with extreme mass ratios. *Mon. Not. R. Astron. Soc.*, **186**(Mar.), 799–812.
- Lin, D. N. C., and Papaloizou, J. 1986. On the tidal interaction between protoplanets and the protoplanetary disk. III - Orbital migration of protoplanets. *Astrophys. J.*, **309**(Oct.), 846–857.
- Lissauer, J. J., Peale, S. J., and Cuzzi, J. N. 1984. Ring torque on Janus and the melting of Enceladus. *Icarus*, **58**(May), 159–168.
- Lissauer, J. J., Dawson, R. I., and Tremaine, S. 2014. Advances in exoplanet science from Kepler. *Nature*, **513**(Sept.), 336–344.
- Lynden-Bell, D., and Pringle, J. E. 1974. The evolution of viscous discs and the origin of the nebular variables. *Mon. Not. R. Astron. Soc.*, **168**(Sept.), 603–637.
- Malhotra, R. 1995. The Origin of Pluto’s Orbit: Implications for the Solar System Beyond Neptune. *Astron. J.*, **110**(July), 420.
- Marley, M. S., Fortney, J. J., Hubickyj, O., Bodenheimer, P., and Lissauer, J. J. 2007. On the Luminosity of Young Jupiters. *Astrophys. J.*, **655**(Jan.), 541–549.
- Martin, R. G., and Livio, M. 2015. The Solar System as an Exoplanetary System. *Astrophys. J.*, **810**(Sept.), 105.
- Meyer-Vernet, N., and Sicardy, B. 1987. On the physics of resonant disk-satellite interaction. *Icarus*, **69**(Jan.), 157–175.
- Morbidelli, A., Tsiganis, K., Batygin, K., Crida, A., and Gomes, R. 2012. Explaining why the uranian satellites have equatorial prograde orbits despite the large planetary obliquity. *Icarus*, **219**(June), 737–740.
- Morfill, G. E., Fechtig, H., Gruen, E., and Goertz, C. K. 1983. Some consequences of meteoroid impacts on Saturn’s rings. *Icarus*, **55**(Sept.), 439–447.
- Mosqueira, I., and Estrada, P. R. 2002. Apse Alignment of the Uranian Rings. *Icarus*, **158**(Aug.), 545–556.
- Mosqueira, I., and Estrada, P. R. 2003a. Formation of the regular satellites of giant planets in an extended gaseous nebula.

- ula I: subnebula model and accretion of satellites. *Icarus*, **163**(May), 198–231.
- Mosqueira, I., and Estrada, P. R. 2003b. Formation of the regular satellites of giant planets in an extended gaseous nebula II: satellite migration and survival. *Icarus*, **163**(May), 232–255.
- Movshovitz, N., Nimmo, F., Korycansky, D. G., Asphaug, E., and Owen, J. M. 2016. Impact disruption of gravity-dominated bodies: New simulation data and scaling. *Icarus*, **275**(Sept.), 85–96.
- Namouni, F., and Porco, C. 2002. The confinement of Neptune’s ring arcs by the moon Galatea. *Nature*, **417**(May), 45–47.
- Nicholson, P. D., Hedman, M. M., Clark, R. N., Showalter, M. R., Cruikshank, D. P., Cuzzi, J. N., Filacchione, G., Capaccioni, F., Cerroni, P., Hansen, G. B., Sicardy, B., Drossart, P., Brown, R. H., Buratti, B. J., Baines, K. H., and Coradini, A. 2008. A close look at Saturn’s rings with Cassini VIMS. *Icarus*, **193**(Jan.), 182–212.
- Northrop, T. G., and Connerney, J. E. P. 1987. A micrometeorite erosion model and the age of Saturn’s rings. *Icarus*, **70**(Apr.), 124–137.
- Ogihara, M., and Ida, S. 2012. N-body Simulations of Satellite Formation around Giant Planets: Origin of Orbital Configuration of the Galilean Moons. *Astrophys. J.*, **753**(July), 60.
- Ortiz, J. L., Duffard, R., Pinilla-Alonso, N., Alvarez-Candal, A., Santos-Sanz, P., Morales, N., Fernández-Valenzuela, E., Licandro, J., Campo Bagatin, A., and Thirouin, A. 2015. Possible ring material around centaur (2060) Chiron. *Astron. Astrophys.*, **576**(Apr.), A18.
- Pan, M., and Wu, Y. 2016. On the Mass and Origin of Chariklo’s Rings. *ApJ*, **821**(Apr.), 18.
- Pollack, J. B. 1975. The rings of Saturn. *Space Sci. Rev.*, **18**(Oct.), 3–93.
- Pollack, J. B. 1976 (Mar.). *Evolution of Jupiter, Saturn and Their Satellite Systems*. Tech. rept. NASA.
- Pollack, J. B., Grossman, A. S., Moore, R., and Graboske, Jr., H. C. 1977. A calculation of Saturn’s gravitational contraction history. *Icarus*, **30**(Jan.), 111–128.
- Porco, C. C. 1991. An explanation for Neptune’s ring arcs. *Science*, **253**(Aug.), 995–1001.
- Porco, C. C., and Goldreich, P. 1987. Shepherding of the Uranian rings. I - Kinematics. *Astron. J.*, **93**(Mar.), 724–737.
- Porco, C. C., Helfenstein, P., Thomas, P. C., Ingersoll, A. P., Wisdom, J., West, R., Neukum, G., Denk, T., Wagner, R., Roatsch, T., Kieffer, S., Turtle, E., McEwen, A., Johnson, T. V., Rathbun, J., Veverka, J., Wilson, D., Perry, J., Spitale, J., Brahic, A., Burns, J. A., Del Genio, A. D., Dones, L., Murray, C. D., and Squyres, S. 2006. Cassini Observes the Active South Pole of Enceladus. *Science*, **311**(Mar.), 1393–1401.
- Poulet, F., and Sicardy, B. 2001. Dynamical evolution of the Prometheus-Pandora system. *Mon. Not. R. Astron. Soc.*, **322**(Apr.), 343–355.
- Pringle, J. E. 1981. Accretion discs in astrophysics. *Annu. Rev. Astron. Astrophys.*, **19**, 137–162.
- Reffet, E., Verdier, M., and Ferrari, C. 2015. Thickness of Saturn’s B ring as derived from seasonal temperature variations measured by Cassini CIRS. *Icarus*, **254**(July), 276–286.
- Rice, W. K. M., and Armitage, P. J. 2009. Time-dependent models of the structure and stability of self-gravitating protoplanetary discs. *Mon. Not. R. Astron. Soc.*, **396**(July), 2228–2236.
- Robbins, S. J., Stewart, G. R., Lewis, M. C., Colwell, J. E., and Sremčević, M. 2010. Estimating the masses of Saturn’s A and B rings from high-optical depth N-body simulations and stellar occultations. *Icarus*, **206**(Apr.), 431–445.
- Roche, Édouard. 1849. *Mémoire sur la figure d’une masse fluide, soumise à l’attraction d’un point éloigné*. Mémoire de la section des sciences, Académie des sciences et des lettres de Montpellier, 1, 243.
- Rosenblatt, P., and Charnoz, S. 2012. On the formation of the martian moons from a circum-martian accretion disk. *Icarus*, **221**(Nov.), 806–815.
- Rosenblatt, P., Charnoz, S., Dunseath, K., Terao-Dunseath, M., Trinh, A., Hyodo, R., Genda, H., and Toupin, S. 2016. Accretion of Phobos and Deimos in an extended debris disc stirred by transient moons. *Nature Geosci.*, **9**(July), 581–583.
- Ruprecht, J. D., Bosh, A. S., Person, M. J., Bianco, F. B., Fulton, B. J., Gulbis, A. A. S., Bus, S. J., and Zangari, A. M. 2015. 29 November 2011 stellar occultation by 2060 Chiron: Symmetric jet-like features. *Icarus*, **252**(May), 271–276.
- Salmon, J., and Canup, R. M. 2014 (Nov.). Forming Inner Ice-Rich Moons at Saturn from a Massive Early Ring. Page 501.08 of: *AAS/Division for Planetary Sciences Meeting Abstracts*. AAS/Division for Planetary Sciences Meeting Abstracts, vol. 46.
- Salmon, J., and Canup, R. M. 2015 (Nov.). Strong orbital expansion of Saturn’s inner ice-rich moons through ring torques and mutual resonances during their accretion from a massive ring. Page 104.08 of: *AAS/Division for Planetary Sciences Meeting Abstracts*. AAS/Division for Planetary Sciences Meeting Abstracts, vol. 47.
- Salmon, J., and Canup, R. M. 2016. . *Icarus*, submitted.
- Salmon, J., Charnoz, S., Crida, A., and Brahic, A. 2010. Long-term and large-scale viscous evolution of dense planetary rings. *Icarus*, **209**(Oct.), 771–785.
- Sasaki, T., Stewart, G. R., and Ida, S. 2010. Origin of the Different Architectures of the Jovian and Saturnian Satellite Systems. *Astrophys. J.*, **714**(May), 1052–1064.
- Showalter, M. R., Cheng, A. F., Weaver, H. A., Stern, S. A., Spencer, J. R., Throop, H. B., Birath, E. M., Rose, D., and Moore, J. M. 2007. Clump Detections and Limits on Moons in Jupiter’s Ring System. *Science*, **318**(Oct.), 232.
- Sicardy, B., Roddier, F., Roddier, C., Perozzi, E., Graves, J. E., Guyon, O., and Northcott, M. J. 1999. Images of Neptune’s ring arcs obtained by a ground-based telescope. *Nature*, **400**(Aug.), 731–733.
- Slattery, W. L. 1992. Giant impacts on a primitive Uranus. *Icarus*, **99**(Sept.), 167–174.
- Sridhar, S., and Tremaine, S. 1992. Tidal disruption of viscous bodies. *Icarus*, **95**(Jan.), 86–99.
- Throop, H. B., Porco, C. C., West, R. A., Burns, J. A., Showalter, M. R., and Nicholson, P. D. 2004. The jovian rings: new results derived from Cassini, Galileo, Voyager, and Earth-based observations. *Icarus*, **172**(Nov.), 59–77.
- Tiscareno, M. S., Burns, J. A., Nicholson, P. D., Hedman, M. M., and Porco, C. C. 2007. Cassini imaging of Saturn’s rings. II. A wavelet technique for analysis of density waves and other radial structure in the rings. *Icarus*, **189**(July), 14–34.
- Tiscareno, M. S., Mitchell, C. J., Murray, C. D., Di Nino, D., Hedman, M. M., Schmidt, J., Burns, J. A., Cuzzi, J. N., Porco, C. C., Beurle, K., and Evans, M. W. 2013a. Observations of Ejecta Clouds Produced by Impacts onto Saturn’s Rings. *Science*, **340**(Apr.), 460–464.
- Tiscareno, M. S., Hedman, M. M., Burns, J. A., Weiss, J. W., and Porco, C. C. 2013b. Probing the inner boundaries of Saturn’s A ring with the Iapetus -1:0 nodal bending wave. *Icarus*, **224**(May), 201–208.



- Toomre, A. 1964. On the gravitational stability of a disk of stars. *Astrophys. J.*, **139**(May), 1217–1238.
- Tremaine, S., Touma, J., and Namouni, F. 2009. Satellite Dynamics on the Laplace Surface. *Astron. J.*, **137**(Mar.), 3706–3717.
- Ward, W. R. 1984. The solar nebula and the planetesimal disk. Pages 660–684 of: Greenberg, R., and Brahic, A. (eds), *IAU Colloq. 75: Planetary Rings*.
- Ward, W. R. 1986. Density waves in the solar nebula - Differential Lindblad torque. *Icarus*, **67**(July), 164–180.
- Ward, W. R., and Canup, R. M. 2010. Circumplanetary Disk Formation. *Astron. J.*, **140**(Nov.), 1168–1193.
- Weidenschilling, S. J., and Cuzzi, J. N. 1993. Formation of planetesimals in the solar nebula. Pages 1031–1060 of: Levy, E. H., and Lunine, J. I. (eds), *Protostars and Planets III*.
- Weidenschilling, S. J., Chapman, C. R., Davis, D. R., and Greenberg, R. 1984. Ring particles - Collisional interactions and physical nature. Pages 367–415 of: Greenberg, R., and Brahic, A. (eds), *IAU Colloq. 75: Planetary Rings*.
- Yoder, C. F. 1995. Astrometric and Geodetic Properties of Earth and the Solar System. Page 1 of: Ahrens, T. J. (ed), *Global Earth Physics: A Handbook of Physical Constants*.
- Zahnle, K., Schenk, P., Levison, H., and Dones, L. 2003. Cratering rates in the outer Solar System. *Icarus*, **163**(June), 263–289.
- Zebker, H. A., and Tyler, G. L. 1984. Thickness of Saturn's rings inferred from Voyager 1 observations of microwave scatter. *Science*, **223**(Jan.), 396–398.
- Zhang, Z., Hayes, A. G., Janssen, M. A., Nicholson, P. D., Cuzzi, J. N., de Pater, I., Dunn, D. E., Estrada, P. R., and Hedman, M. M. 2017. Cassini microwave observations provide clues to the origin of Saturn's C ring. *Icarus*, **281**(Jan.), 297–321.